J|A|C|S
ARTICLES
Published on Web 05/18/2007

Triplet Reactivity and Regio-/Stereoselectivity in the Macrocyclization of Diastereomeric Ketoprofen−Quencher Conjugates *via* Remote Hydrogen Abstractions

Sergio Abad,[†] Francisco Boscá,[†] Luis R. Domingo,[‡] Salvador Gil,[‡] Uwe Pischel,[†] and Miguel A. Miranda*,[†]

Instituto de Tecnología Química, UPV-CSIC, Universidad Politécnica de Valencia, Av. de los Naranjos s/n, E-46022 Valencia, Spain, and Departamento de Química Orgánica, Universidad de Valencia, Dr. Moliner 50, E-46100 Burjassot (Valencia), Spain

Received February 22, 2007; E-mail: mmiranda@qim.upv.es

Abstract: Intramolecular excited triplet state interactions in diastereomeric compounds composed of a benzophenone chromophore (ketoprofen) and various hydrogen donor moieties (tetrahydrofuran, isopropylbenzene) have been investigated by laser flash photolysis. The rate constants for hydrogen abstraction by excited triplet benzophenone are in the order of 10^4-10^5 s^{-1}, with the highest reactivity for the tetrahydrofuran residue. A remarkable diastereodifferentiation, expressed in the triplet lifetimes of the carbonyl chromophore (e.g., 1.6 *versus* 2.7 μs), has been found for these compounds. With an alkylaromatic moiety as donor, related effects have been observed, albeit strongly dependent on the length of the spacer. The reactivity trend for the initial hydrogen transfer step is paralleled by the quantum yields of the overall photoreaction. The biradicals, formed *via* remote hydrogen abstraction, undergo intramolecular recombination to macrocyclic ring systems. The new photoproducts have been isolated and characterized by NMR spectroscopy. The stereochemistry of the macrocycles, which contain up to four asymmetric carbons, has been unambiguously assigned on the basis of single-crystal structures and/or NOE effects. Interestingly, a highly regio- and stereoselective macrocyclization has been found for the ketoprofen−tetrahydrofuran conjugates, where hydrogen abstraction from the less substituted carbon is exclusive; *cisoid* ring junction is always preferred over the *transoid* junction. The photoreaction is less regioselective for compounds with an isopropylbenzene residue. The reactivity and selectivity trends have been rationalized by DFT (B3LYP/6-31G*) calculations.

Introduction

Photoinduced hydrogen abstraction initiated by carbonyl species is one of the most intensively investigated fundamental processes in photochemistry and has traditionally played a key role in the development of the existing knowledge of excited states.[1−6] Different mechanistic aspects of this photoprocess have been considered, including spin multiplicity[7,8] (singlet *versus* triplet) and electronic nature[9,10] (n,π^* *versus* π,π^*) of the excited state. The reactivity of n,π^*-excited triplet aromatic ketones, mostly benzophenone, with alkanes,[11] alcohols,[12] hydrides,[13] alkylbenzenes,[9,14] and amines[15−17] has been investigated to establish the role of the donor in the hydrogen abstraction process.[2,6] This has revealed the involvement of a variety of mechanisms encompassing from "pure" alkoxyl-radical-like abstractions (with alkanes as hydrogen donors) to charge-transfer-initiated reactions (in the case of amines).[6] Other issues such as stereoelectronic and steric hindrance effects[8,18−20] or the influence of the chemical surrounding (solvent polarity, hydrogen bonding) have also been investigated.[8,15,16,21]

[†] Universidad Politécnica de Valencia.
[‡] Universidad de Valencia.

(1) Turro, N. J.; Dalton, J. C.; Dawes, K.; Farrington, G.; Hautala, R.; Morton, D.; Niemczyk, M.; Schore, N. *Acc. Chem. Res.* **1972**, *5*, 92−101.
(2) Scaiano, J. C. *J. Photochem.* **1973**, *2*, 81−118.
(3) Wagner, P. J. *Top. Curr. Chem.* **1976**, *66*, 1−52.
(4) Wagner, P.; Park, B.-S. *Org. Photochem.* **1991**, *11*, 227−366.
(5) Nau, W. M. *Ber. Bunsen. Phys. Chem.* **1998**, *102*, 476−485.
(6) Nau, W. M.; Pischel, U. Photoreactivity of n,π^*-Excited Azoalkanes and Ketones. In *Molecular and Supramolecular Photochemistry*; Ramamurthy, V., Schanze, K., Eds.; Taylor and Francis Group: Boca Raton, FL, 2006; pp 75−129.
(7) Nau, W. M.; Cozens, F. L.; Scaiano, J. C. *J. Am. Chem. Soc.* **1996**, *118*, 2275−2282.
(8) Pischel, U.; Nau, W. M. *J. Am. Chem. Soc.* **2001**, *123*, 9727−9737.
(9) Wagner, P. J.; Truman, R. J.; Puchalski, A. E.; Wake, R. *J. Am. Chem. Soc.* **1986**, *108*, 7727−7738.
(10) Leigh, W. J.; Lathioor, E. C.; St. Pierre, M. J. *J. Am. Chem. Soc.* **1996**, *118*, 12339−12348.
(11) Giering, L.; Berger, M.; Steel, C. *J. Am. Chem. Soc.* **1974**, *96*, 953−958.
(12) Wagner, P. J.; Puchalski, A. E. *J. Am. Chem. Soc.* **1980**, *102*, 7138−7140.
(13) Scaiano, J. C. *J. Am. Chem. Soc.* **1980**, *102*, 5399−5400.
(14) Pischel, U.; Patra, D.; Koner, A. L.; Nau, W. M. *Photochem. Photobiol.* **2006**, *82*, 310−317.
(15) Gorman, A. A.; Parekh, C. T.; Rodgers, M. A. J.; Smith, P. G. *J. Photochem.* **1978**, *9*, 11−17.
(16) Parola, A. H.; Cohen, S. G. *J. Photochem.* **1980**, *12*, 41−50.
(17) Inbar, S.; Linschitz, H.; Cohen, S. G. *J. Am. Chem. Soc.* **1981**, *103*, 1048−1054.
(18) Griller, D.; Howard, J. A.; Marriott, P. R.; Scaiano, J. C. *J. Am. Chem. Soc.* **1981**, *103*, 619−623.
(19) von Raumer, M.; Suppan, P.; Haselbach, E. *Helv. Chim. Acta* **1997**, *80*, 719−724.
(20) Pischel, U.; Zhang, X.; Hellrung, B.; Haselbach, E.; Muller, P.-A.; Nau, W. M. *J. Am. Chem. Soc.* **2000**, *122*, 2027−2034.
(21) Nau, W. M.; Pischel, U. *Angew. Chem., Int. Ed.* **1999**, *38*, 2885−2888.

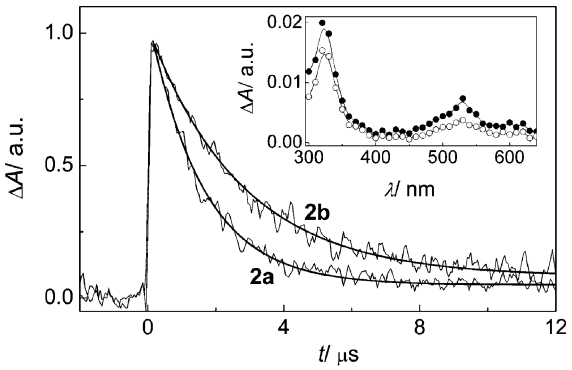

Figure 1. Normalized triplet−triplet absorption decay traces ($\lambda_{obsd} = 530$ nm) of **2a** and **2b** obtained upon excitation at 266 nm in N_2-outgassed acetonitrile and corresponding monoexponential fits (solid lines). The inset shows the transient absorption spectra obtained for **2a** at different delay times after the laser pulse [0.1 μs (●) and 1.0 μs (○)].

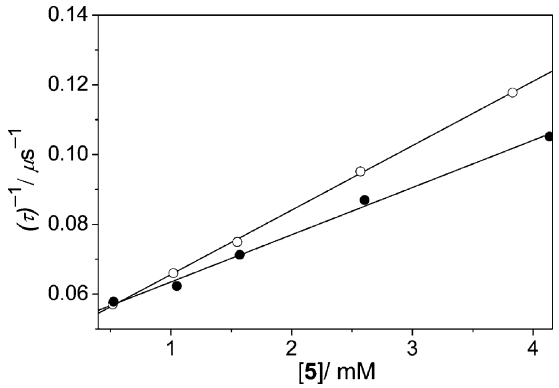

Figure 2. Kinetic plot for the triplet quenching of **1** by **5a** (○) or **5b** (●). The data were obtained for $\lambda_{obsd} = 530$ nm upon excitation at 266 nm in N_2-outgassed acetonitrile.

Besides, the contribution of carbonyl photoreduction to the development of molecular organic photochemistry is not merely restricted to the mechanistic field. Since early reports on intramolecular carbon−carbon bond-forming reactions after intramolecular hydrogen abstraction by a photoexcited ketone,[22] the process has evolved as an important tool in synthetic organic photochemistry for preparation of small rings (three-, four-, and five-membered)[23−33] and large macrocycles.[34−41] The primary

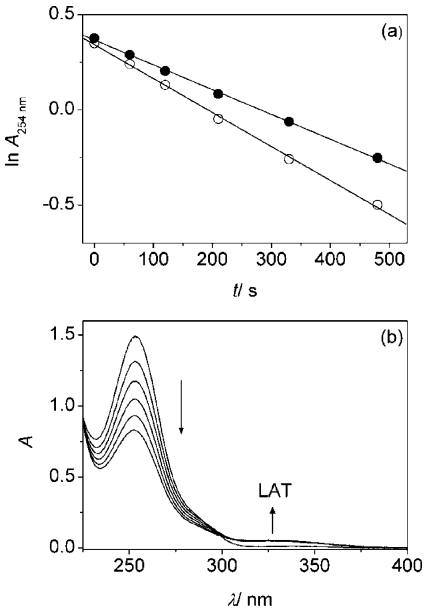

Figure 3. (a) Logarithmic plot of the absorbance at 254 nm of **2a** (○) and **2b** (●) against the irradiation time *t*. (b) Corresponding temporal development (0, 60, 120, 210, 330, and 480 s irradiation time) of the UV/vis absorption spectra of **2a** in N_2-outgassed acetonitrile.

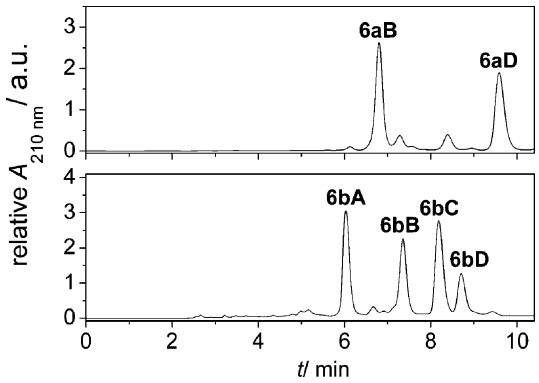

Figure 4. HPLC chromatograms of the mixtures obtained by irradiation of **2a** (top) and **2b** (bottom).

intermediates are 1,*n*-biradicals, and the ring size is determined by the distance between the hydrogen donor and acceptor sites. Biradical dynamics has been recognized to be very important in a variety of thermal and photochemical reactions[32,42−44] and has a high impact on the stereoselectivity of the cyclization reaction, where two new stereogenic centers may be formed. Indeed, the stereoselectivity of this type of reaction, both in the solid state and in solution, has been thoroughly studied with special emphasis on chiral memory and asymmetric induction phenomena.[23−28,33,44,45]

However, although directly related to asymmetric photoreactions,[46,47] diastereodifferentiation in the intramolecular quenching of excited states (that controls the kinetics of photoprocesses such as exciplex formation, hydrogen abstraction, or electron

(22) Yang, N. C.; Yang, D.-D. H. *J. Am. Chem. Soc.* **1958**, *80*, 2913−2914.
(23) Bach, T.; Aechtner, T.; Neumüller, B. *Chem.—Eur. J.* **2002**, *8*, 2464−2475.
(24) Braga, D.; Chen, S.; Filson, H.; Maini, L.; Netherton, M. R.; Patrick, B. O.; Scheffer, J. R.; Scott, C.; Xia, W. *J. Am. Chem. Soc.* **2004**, *126*, 3511−3520.
(25) Giese, B.; Wettstein, P.; Stähelin, C.; Barbosa, F.; Neuburger, M.; Zehnder, M.; Wessig, P. *Angew. Chem., Int. Ed.* **1999**, *38*, 2586−2587.
(26) Griesbeck, A. G.; Heckroth, H. *J. Am. Chem. Soc.* **2002**, *124*, 396−403.
(27) Griesbeck, A. G.; Heckroth, H.; Lex, J. *Chem. Commun.* **1999**, 1109−1110.
(28) Gudmundsdottir, A. D.; Lewis, T. J.; Randall, L. H.; Scheffer, J. R.; Rettig, S. J.; Trotter, J.; Wu, C.-H. *J. Am. Chem. Soc.* **1996**, *118*, 6167−6184.
(29) Leibovitch, M.; Olovsson, G.; Scheffer, J. R.; Trotter, J. *J. Am. Chem. Soc.* **1998**, *120*, 12755−12769.
(30) Patrick, B. O.; Scheffer, J. R.; Scott, C. *Angew. Chem., Int. Ed.* **2003**, *42*, 3775−3777.
(31) Vishnumurthy, K.; Cheung, E.; Scheffer, J. R.; Scott, C. *Org. Lett.* **2002**, *4*, 1071−1074.
(32) Wagner, P. J. *Acc. Chem. Res.* **1989**, *22*, 83−91.
(33) Zand, A.; Park, B.-S.; Wagner, P. J. *J. Org. Chem.* **1997**, *62*, 2326−2327.
(34) Breslow, R.; Winnik, M. A. *J. Am. Chem. Soc.* **1969**, *91*, 3083−3084.
(35) Baldwin, J. E.; Bhatnagar, A. K.; Harper, R. W. *J. Chem. Soc., Chem. Commun.* **1970**, 659−661.
(36) Breslow, R.; Baldwin, S. W. *J. Am. Chem. Soc.* **1970**, *92*, 732−734.
(37) Breslow, R.; Kalicky, P. *J. Am. Chem. Soc.* **1971**, *93*, 3540−3541.
(38) Paquette, L. A.; Balogh, D. W. *J. Am. Chem. Soc.* **1982**, *104*, 774−783.
(39) Wagner, P. J. *Acc. Chem. Res.* **1983**, *16*, 461−467.
(40) Sugimura, T.; Paquette, L. A. *J. Am. Chem. Soc.* **1987**, *109*, 3017−3024.
(41) Griesbeck, A. G.; Henz, A.; Hirt, J. *Synthesis* **1996**, *11*, 1261−1276.
(42) Doubleday, C., Jr.; Turro, N. J.; Wang, J.-F. *Acc. Chem. Res.* **1989**, *22*, 199−205.
(43) Johnston, L. J.; Scaiano, J. C. *Chem. Rev.* **1989**, *89*, 521−547.
(44) Griesbeck, A. G.; Mauder, H.; Stadtmüller, S. *Acc. Chem. Res.* **1994**, *27*, 70−75.
(45) Natarajan, A.; Mague, J. T.; Ramamurthy, V. *J. Am. Chem. Soc.* **2005**, *127*, 3568−3576.
(46) Rau, H. *Chem. Rev.* **1983**, *83*, 535−547.
(47) Inoue, Y. *Chem. Rev.* **1992**, *92*, 741−770.

Chart 1

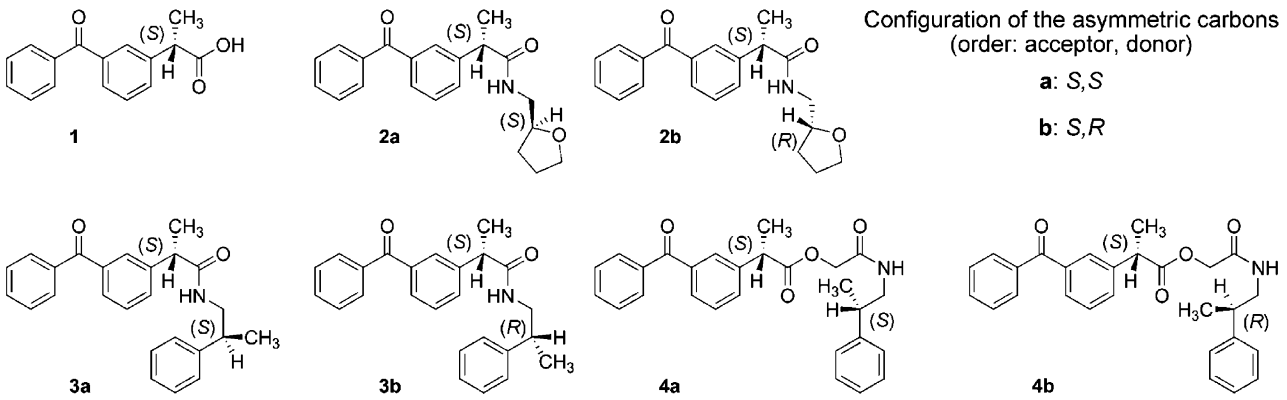

Table 1. Photophysical and Photochemical Data of Diastereomeric Ketoprofen−Quencher Conjugates **2a**,**b**−**4a**,**b**

conjugate[a]	τ_T[b]/μs	$k_H \times 10^{-5}$[c]/s^{-1}	Φ_r[d]
2a	1.6	5.9	0.21
2b	2.7	3.2	0.15
3a	15.0	0.23	<0.05
3b	12.2	0.38	<0.01
4a	4.5	1.8	0.18
4b	5.1	1.5	0.15

[a] Stereochemistry of the asymmetric carbons: *S*,*S* (**a**), *S*,*R* (**b**), see also Chart 1. [b]Triplet lifetimes in acetonitrile measured at $\lambda_{obsd} = 530$ nm upon excitation at 266 nm. [c]Rate constants of hydrogen abstraction obtained with eq 1. [d]Photoreaction quantum yields in acetonitrile ($\lambda_{exc} = 254$ nm); phenylglyoxylic acid was used as actinometer (*cf.* ref 76).

Chart 2

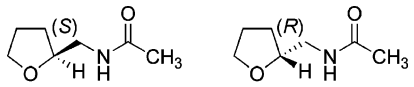

transfer) has been much less frequently observed.[48−58] Specifically, diastereodifferentiating interactions in the intramolecular hydrogen abstraction by excited triplet aromatic ketones from different donors have been rarely reported.[52−54,57,58]

On the other hand, stereodifferentiating interactions in the excited state have relevant implications in biological systems. Phototoxicity and photoallergy are subjects of increasing interest in medicine and toxicology; they cause drug-photosensitized damage to target biomolecules (such as proteins, lipids, or DNA) occurring through a variety of mechanisms.[59] As already known

Table 2. Chemical Yields of the Photoproducts Obtained upon Irradiation of the Ketoprofen−Quencher Conjugates

conjugate		product yield (%)			
		A	**B**	**C**	**D**
2a	**6a**		38		36
2b	**6b**	25	20	27	13
4a	**7a**	21	27		
4a	**8**	10	11	11	10
4b	**7b**	10	14	20	13
4b	**8**	8	9	9	8

for other undesired side-effects, phototoxicity and photoallergy may be stereoselective, so that the benefit/risk ratio may be different for the two drug enantiomers. In this context, we have recently reported on the interactions between photosensitizing chiral drugs and proteins or DNA nucleobases.[60−63] Despite the high relevance of such interactions to the biological problem, their study often turns out to be very difficult and requires consideration of a complex combination of factors. Hence, in many cases it has been found to be advantageous to use models, where the drug chromophores and key substrates of the biomolecules are covalently linked.[50,52−54,56,62−64] Thus, supramolecular interactions in the real complexes are mimicked by intramolecular interactions in model compounds.

With this background, we have now synthesized a series of diastereomeric compounds **2a**,**b**−**4a**,**b** combining (*S*)-ketoprofen (**1**) and chiral hydrogen donors (*cf.* Chart 1). Ketoprofen is an established photosensitizer, containing the benzophenone chromophore, whose photophysics and photochemistry are well-characterized.[65−67] Further, it is a 2-arylpropionic acid, used as a nonsteroidal anti-inflammatory drug, which has been investigated in connection with its potential to mediate photoallergic and phototoxic effects.[68,69] Tetrahydrofuran and alkylbenzenes

(48) Boch, R.; Bohne, C.; Scaiano, J. C. *J. Org. Chem.* **1996**, *61*, 1423−1428.
(49) Moorthy, J. N.; Patterson, W. S.; Bohne, C. *J. Am. Chem. Soc.* **1997**, *119*, 11094−11095.
(50) Miranda, M. A.; Lahoz, A.; Martínez-Máñez, R.; Boscá, F.; Castell, J. V.; Pérez-Prieto, J. *J. Am. Chem. Soc.* **1999**, *121*, 11569−11570.
(51) Moorthy, J. N.; Monahan, S. L.; Sunoj, R. B.; Chandrasekhar, J.; Bohne, C. *J. Am. Chem. Soc.* **1999**, *121*, 3093−3103.
(52) Miranda, M. A.; Martínez, L. A.; Samadi, A.; Boscá, F.; Morera, I. M. *Chem. Commun.* **2002**, 280−281.
(53) Boscá, F.; Andreu, I.; Morera, I. M.; Samadi, A.; Miranda, M. A. *Chem. Commun.* **2003**, 1592−1593.
(54) Pischel, U.; Abad, S.; Domingo, L. R.; Boscá, F.; Miranda, M. A. *Angew. Chem., Int. Ed.* **2003**, *42*, 2531−2534.
(55) Pischel, U.; Abad, S.; Miranda, M. A. *Chem. Commun.* **2003**, 1088−1089.
(56) Pérez-Prieto, J.; Lahoz, A.; Boscá, F.; Martínez-Máñez, R.; Miranda, M. A. *J. Org. Chem.* **2004**, *69*, 374−381.
(57) Singhal, N.; Koner, A. L.; Mal, P.; Venugopalan, P.; Nau, W. M.; Moorthy, J. N. *J. Am. Chem. Soc.* **2005**, *127*, 14375−14382.
(58) Samanta, S.; Mishra, B. K.; Pace, T. C. S.; Sathyamurthy, N.; Bohne, C.; Moorthy, J. N. *J. Org. Chem.* **2006**, *71*, 4453−4459.
(59) Spikes, J. D. Photosensitization. In *The Science of Photobiology*, 2nd ed.; Smith, K. C., Ed. Plenum Press: New York, 1989; pp 79−110.
(60) Lhiaubet-Vallet, V.; Sarabia, Z.; Boscá, F.; Miranda, M. A. *J. Am. Chem. Soc.* **2004**, *126*, 9538−9539.
(61) Lhiaubet-Vallet, V.; Encinas, S.; Miranda, M. A. *J. Am. Chem. Soc.* **2005**, *127*, 12774−12775.
(62) Belmadoui, N.; Encinas, S.; Climent, M. J.; Gil, S.; Miranda, M. A. *Chem.−Eur. J.* **2006**, *12*, 553−561.
(63) Lhiaubet-Vallet, V.; Boscá, F.; Miranda, M. A. *J. Phys. Chem. B* **2007**, *111*, 423−431.
(64) Andreu, I.; Boscá, F.; Sanchez, L.; Morera, I. M.; Camps, P.; Miranda, M. A. *Org. Lett.* **2006**, *8*, 4597−4600.
(65) Martínez, L. J.; Scaiano, J. C. *J. Am. Chem. Soc.* **1997**, *119*, 11066−11070.
(66) Monti, S.; Sortino, S.; De Guidi, G.; Marconi, G. *J. Chem. Soc., Faraday Trans.* **1997**, *93*, 2269−2275.
(67) Boscá, F.; Marín, M. L.; Miranda, M. A. *Photochem. Photobiol.* **2001**, *74*, 637−655.
(68) Gould, J. W.; Mercurio, M. G.; Elmets, C. A. *J. Am. Acad. Dermatol.* **1995**, *33*, 551−573.

Scheme 1. Simplified Overview of Relevant Mechanistic Pathways upon Excitation of Ketoprofen−Hydrogen Donor Conjugates[a]

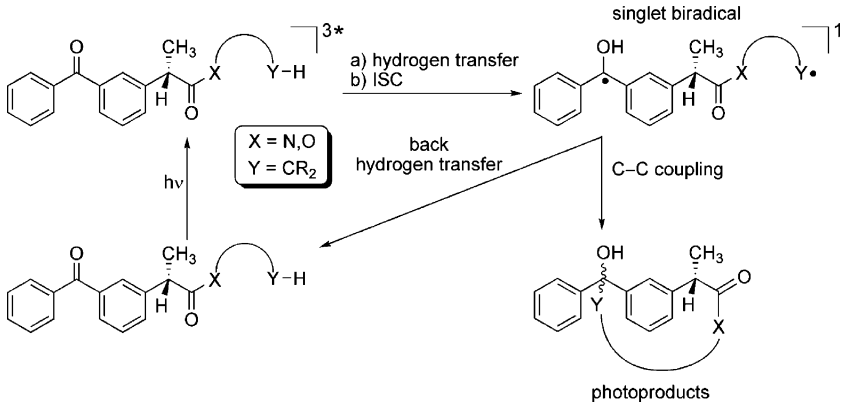

[a] The primary formation of the excited singlet compounds upon light absorption is omitted. ISC: intersystem crossing.

Scheme 2. Structure and Stereochemistry of Photoproducts Obtained from Irradiation of **2a** and **2b**

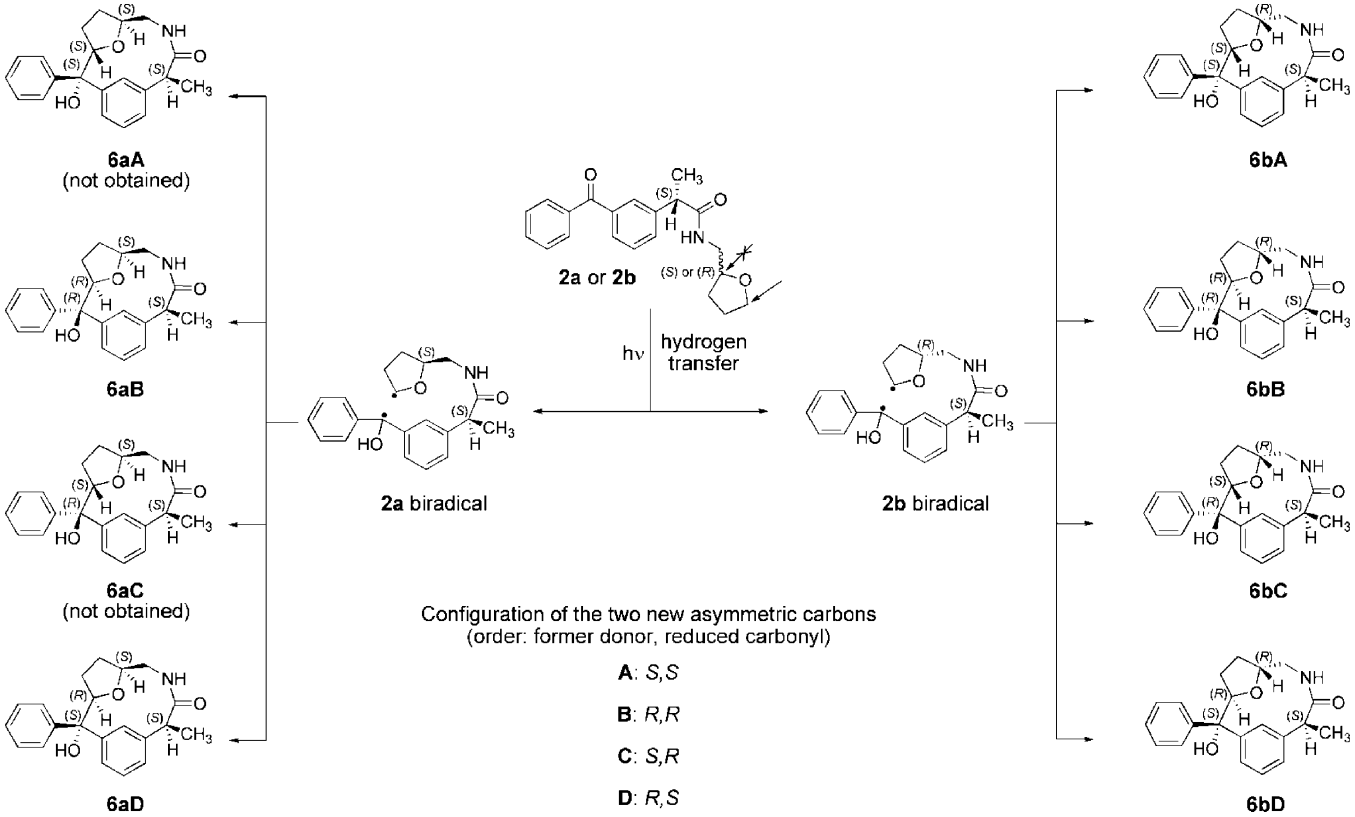

are classical hydrogen donors[6] that have been chosen because they are simple models of more complex components of biomolecules, such as the sugar moiety of nucleic acids or aromatic amino acids.

Hence, laser flash photolysis (LFP) and steady-state irradiation of the ketoprofen−quencher conjugates have been performed in order to gain deeper insight into the role of the donor, the linker, and the chiral information in the primary intramolecular hydrogen abstraction step, as well as in the overall photoprocess. Part of the results were the subject of a preliminary communication.[54] Now we wish to report our results in full, including the synthesis and photochemical investigation of additional conjugates, as well as a comprehensive structural assignment of the photoproducts by NMR spectroscopy and X-ray crystallography. The obtained experimental results in combination with complementary computational DFT studies have allowed us to establish a detailed picture of the regio- and diastereoselectivity associated with the underlying photochemical processes.

Results and Discussion

Diastereodifferentiation in Triplet State Quenching and Photoreaction Quantum Yields. The compounds were prepared from (*S*)-ketoprofen (**1**) or its derivatives and the appropriate chiral amines following standard procedures (*cf.* Experimental Section). They were submitted to laser flash photolysis (λ_{exc} = 266 nm) in order to test the photoreactivity of their excited triplet state in hydrogen abstraction. At the chosen excitation wavelength self-quenching was minimized,

(69) Neumann, N. J.; Holzle, E.; Plewig, G.; Schwarz, T.; Panizzon, R. G.; Breit, R.; Ruzicka, T.; Lehmann, P. *J. Am. Acad. Dermatol.* **2000**, *42*, 183−192.

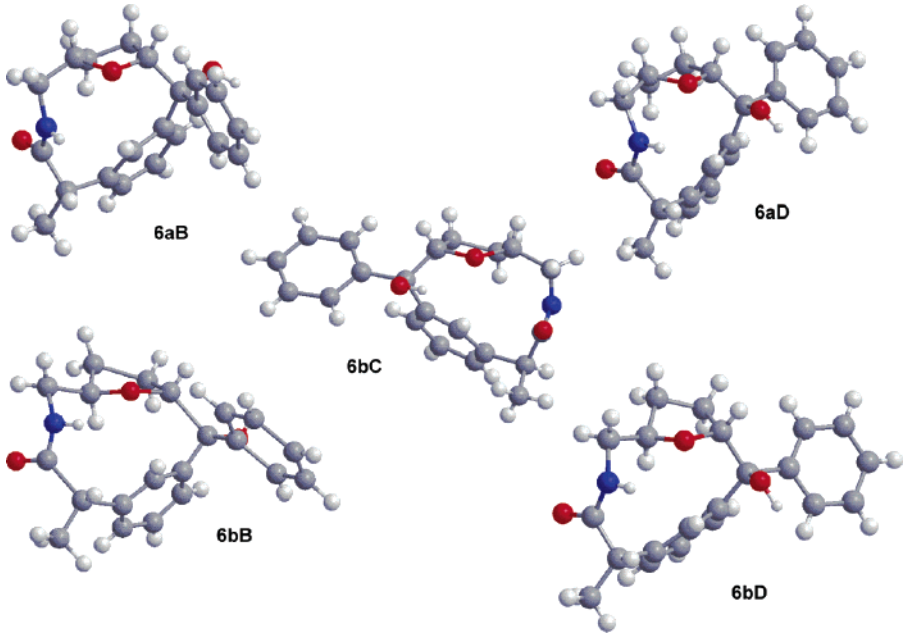

Figure 5. X-ray structures of photoproducts **6aB**, **6aD**, and **6bB**−**6bD**.

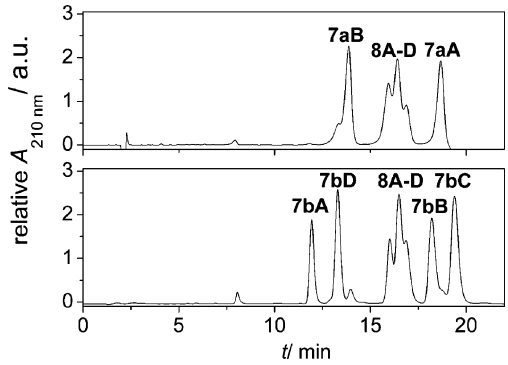

Figure 6. HPLC chromatograms of the product mixtures obtained by irradiation of **4a** (top) and **4b** (bottom) in N_2-outgassed acetonitrile.

which offered the possibility of studying the triplet quenching in a wide dynamic range.

The inset of Figure 1 shows a typical transient absorption spectrum, which was obtained for **2a**. Similar transients with absorption maxima at 325 and 530 nm were detected for all conjugates. The transient was assigned to the excited triplet state (triplet−triplet absorption spectrum) of the benzophenone chromophore, based on the position of the bands and their relative intensities. The ketyl radical (biradical in an intramolecular process) formed by hydrogen abstraction has similar absorption maxima (330 and 540 nm) but would display different relative intensities.[65,67,70] The kinetic analysis of the triplet−triplet absorption spectra was performed at $\lambda_{obsd} = 530$ nm; the obtained lifetimes are compiled in Table 1. Hence, the assignment as biradicals can be further excluded, because they live generally much shorter (sub-microsecond scale) than the observed intermediates in this study (>1.6 μs).[32,43,44] The corresponding transient decay curves for **2a** and **2b** are shown in Figure 1; they revealed a remarkably differentiated kinetic behavior. Clearly, the triplet signal of **2a** decayed significantly faster than that of its stereoisomer **2b**. This difference in the triplet lifetimes must be related with the relative reactivity in photoinduced hydrogen abstraction, pointing to a more efficient process for **2a**. By assuming that this is the only triplet quenching mechanism, the rate constant (k_H) can be determined from the decay times (τ) by means of eq 1, with $\tau_0 = 22.8$ μs being the triplet lifetime of reference compound **1** in the absence of quencher:

$$k_H = 1/\tau - 1/\tau_0 \qquad (1)$$

The role of the hydrogen donor moiety was investigated by introducing **3a** and **3b**, which contain an alkylbenzene moiety as a potential hydrogen donor. Their triplet lifetimes (*cf.* Table 1) were found to be considerably longer than those of **2a** and **2b**; as a consequence the k_H values were 1 order of magnitude smaller, pointing to lower hydrogen transfer reactivity. The hydrogen abstraction rate constants also evidenced a significant stereodifferentiation, with diastereomer **3b** reacting faster than **3a**.

As the benzophenone unit is covalently linked to the donor moiety, the stereodifferentiation must be the result of a delicate balance between three factors: (*i*) the strain introduced in the cyclic transition state for hydrogen abstraction, (*ii*) the steric hindrance related to the close approach between the two active moieties, and (*iii*) the degrees of freedom associated with conformational equilibria. To gain further insight, ketoprofen−alkylbenzene conjugates with a longer spacer (**4a** and **4b**) were investigated. The hydrogen abstraction rate constants were roughly 1 order of magnitude higher than those obtained for **3a** and **3b**. However, no significant reactivity differences between **4a** and **4b** were observed.

In a control experiment we verified whether stereodifferentiation can be also observed in *intermolecular* interactions between (*S*)-ketoprofen **1** and chiral hydrogen donors. The quenching of excited triplet **1** by acetamides **5a** and **5b** (*cf.* Chart 2) was investigated as an example. The reciprocal triplet lifetimes of **1** were plotted against the concentration of compound **5a** or **5b** (*cf.* Figure 2); the bimolecular quenching

(70) Bensasson, R. V.; Gramain, J.-C. *J. Chem. Soc., Faraday Trans.1* **1980**, *76*, 1801−1810.

Scheme 3. Structures of Photoproducts Obtained from Irradiation of **4a** and **4b**[a]

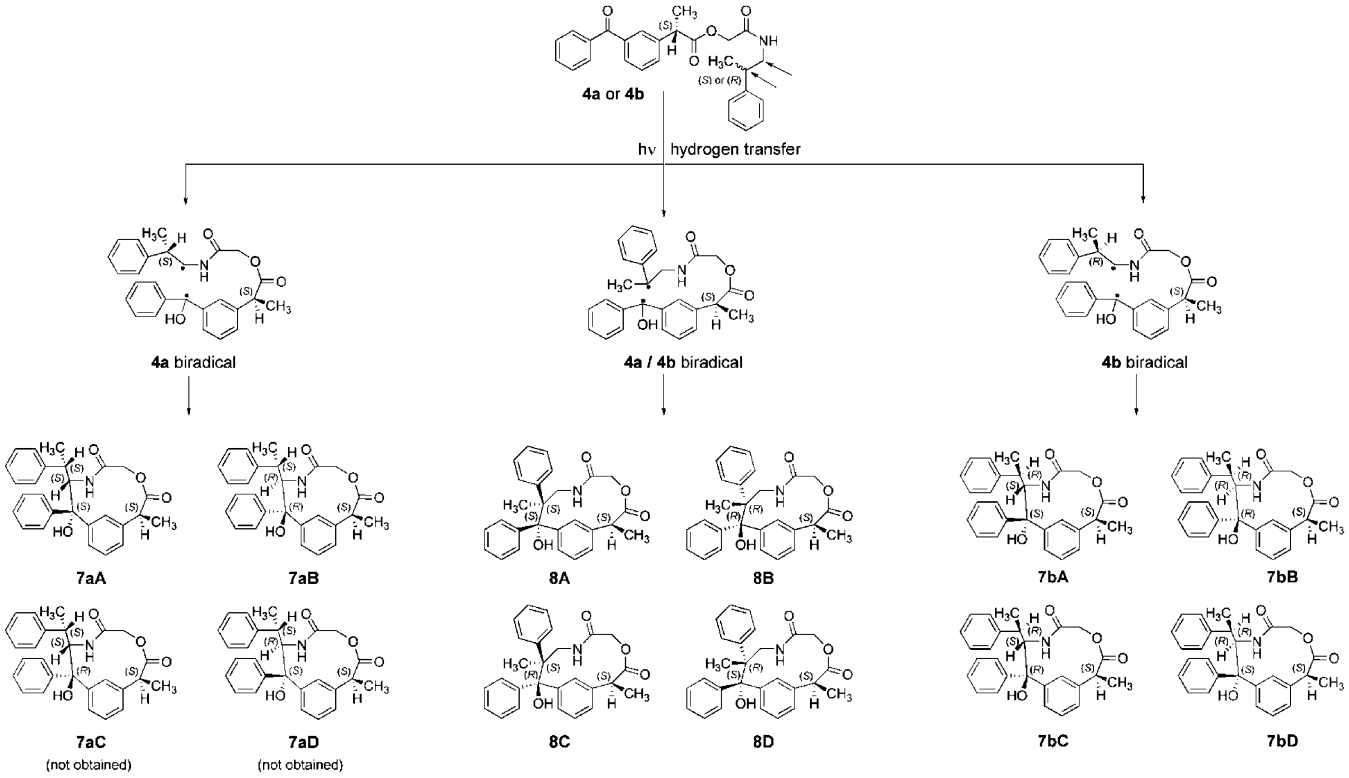

[a] The arrows mark the two positions from where hydrogen atoms are abstracted (capital letter codes are the same as those defined in Scheme 2).

rate constants for hydrogen abstraction were obtained from the slopes according to eq 2:

$$1/\tau = 1/\tau_0 + k_H[\mathbf{5}] \qquad (2)$$

Faster quenching was observed for the *S*,*S* combination, with k_H (**5a**) $= 1.9 \times 10^7$ M^{-1} s^{-1} and k_H (**5b**) $= 1.3 \times 10^7$ M^{-1} s^{-1}.

However, in comparison to the *intramolecular* quenching in **2a** and **2b**, the stereodifferentiation was significantly reduced in the intermolecular quenching experiment as should be expected from the less conditioned approach of both reaction partners. This underlines the importance of the spacer in our experimental approach. Noteworthy, (*S*)-ketoprofen **1** and the acetamides **5** could interact by hydrogen bonding between the carboxy group of **1** and the NH group of **5a** or **5b**. Actually, the ^{1}H NMR titration of **5a** or **5b** with **1** showed pronounced chemical shift changes for the NH protons (*ca*. 0.4 ppm at a ratio 1[**1**]/[**5**] = 3.5). The binding constants fitted according to a 1:1 model were virtually the same for both enantiomers (58 M^{-1} for **5a** and 55 M^{-1} for **5b**)[71] and support the assumption of weak intermolecular interactions with **1**.

As outlined above, diastereodifferentiation in intramolecular hydrogen abstraction by the excited triplet benzophenone chromophore was inferred from the LFP studies. Hence, it was considered interesting to check whether a similar diastereodifferentiation can be observed in the photoreaction quantum yields. For this purpose, the consumption of the conjugates was followed by the disappearance of the benzophenone π,π^* absorption band during steady-state irradiation at 254 nm. Figure 3b shows, as an example, the UV/vis absorption spectra of **2a** after controlled irradiation periods. Note the appearance of a light absorption transient (LAT) as a weak band at *ca.* 330 nm, which is typical for hydrogen abstractions by benzophenone.[72,73] Logarithmic plots of the absorbance at 254 nm against time yielded straight lines (*cf.* Figure 3a), whose slopes were used for estimating the photoreaction quantum yields (Φ_r); they are given in Table 1. In general, the Φ_r values follow the same trend as the triplet quenching, in accordance with the prevailing role of hydrogen abstraction in the quenching process. Thus, the highest photolysis quantum yield ($\Phi_r = 0.21$) was measured for **2a**, for which also the fastest triplet quenching was observed by LFP ($k_H = 5.9 \times 10^5$ s^{-1}). On the other hand, the conjugates with the lowest quenching rate constants, i.e., **3a** and **3b** ($(2.3-3.8) \times 10^4$ s^{-1}), are virtually unreactive ($\Phi_r < 0.05$). Remarkably, the quantum yields also indicate a significant stereodifferentiation in the photoreaction efficiency, which is especially evident for the ketoprofen-tetrahydrofuran conjugates (*cf.* Figure 3a for a comparison between **2a** and **2b**).

Isolation, Identification, and Stereochemical Assignment of the Photoproducts. The intramolecular photoinduced hydrogen transfer in the ketoprofen−quencher conjugates is expected to generate carbon-centered biradicals, which can recombine to form stable macrocyclic C−C coupling products or revert to the starting materials *via* back hydrogen transfer, as shown in Scheme 1.

(71) The binding constants were calculated by fitting of the NMR titration data, using the NMRTit software (download available from http://seitai.chemistry.or.jp/).

(72) Light absorbing transients (LATs) are side products in hydrogen abstraction processes involving benzophenone, which have high extinction coefficients. We presume that in our case they result from the intramolecular attack of the tetrahydrofuranyl radical at the *para*-position of the closest aromatic ring of the ketyl radical. This yields a 1-(phenylhydroxymethylene)-2,5-cyclohexadiene derivative. On the other hand, because of the low concentrations of the conjugates (*ca.* 10^{-4} M), the intermolecular formation of LAT appears rather unlikely.

(73) Filipescu, N.; Minn, F. L. *J. Am. Chem. Soc.* **1968**, *90*, 1544−1547.

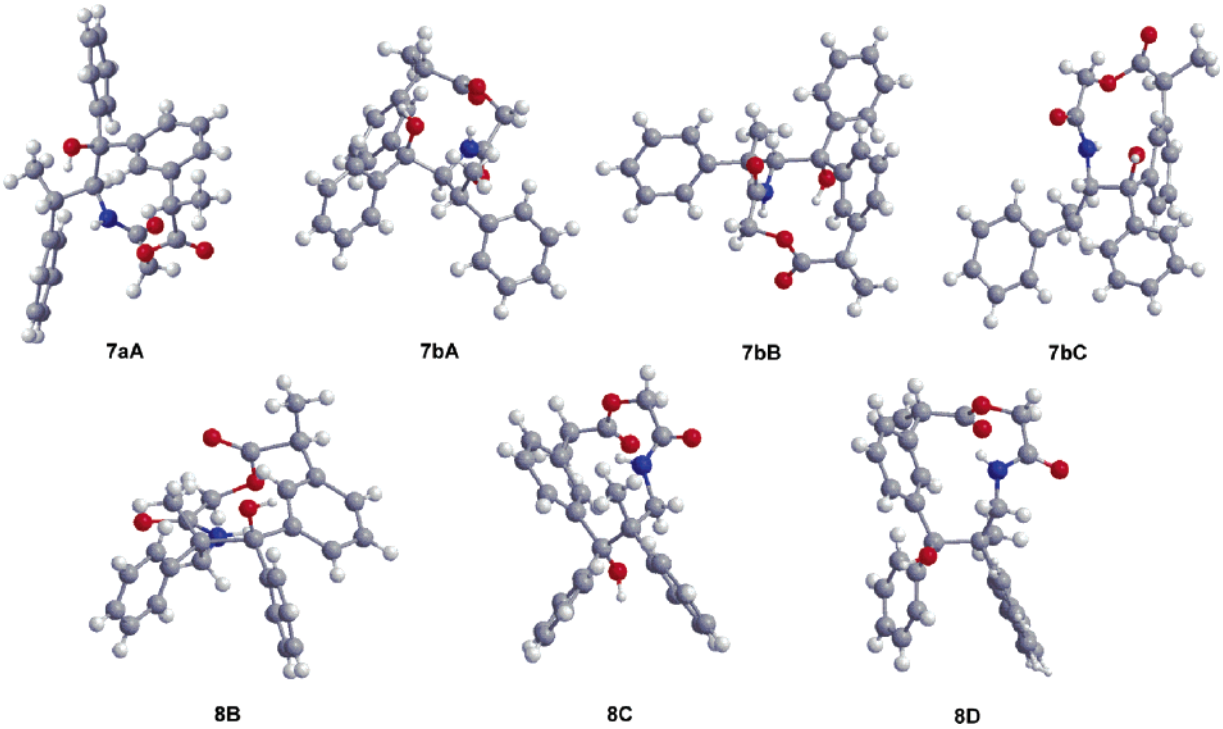

Figure 7. X-ray structures of photoproducts **7aA**, **7bA**−**7bC**, and **8B**−**D**.

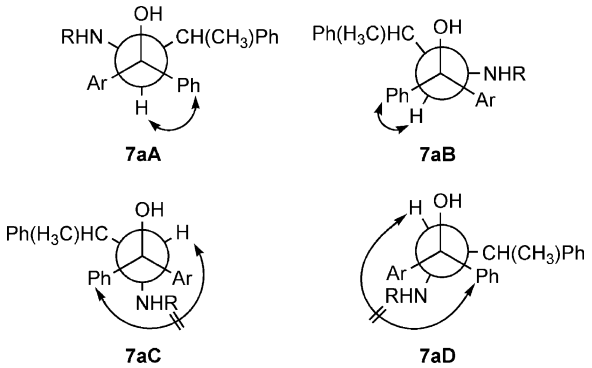

Figure 8. Diagnostic NOE interactions in compounds **7aA**−**7aD**.

Therefore, once the influence of stereochemistry on the reactivity of the conjugates in the hydrogen abstraction process was established, a systematic analysis of the photoproducts was performed. Thus, the ketoprofen−tetrahydrofuran conjugates **2a** and **2b** were irradiated at a preparative scale, and the progress of the photoreactions was followed by HPLC (UV or MS detection). The consumption of the conjugates was accompanied by the formation of several photoproducts. In the case of **2a**, two major peaks, corresponding to **6aB** and **6aD**, appeared in the chromatogram [*cf.* Figure 4 (top) and Scheme 2]. By contrast, four major products (**6bA**, **6bB**, **6bC**, and **6bD**) were obtained upon irradiation of **2b** [*cf.* Figure 4 (bottom)]. The electrospray ionization mass spectra (MS-ES, positive mode) confirmed that these products and the starting compounds were isobaric ([MH^+], $m/z = 338$).

Additionally, the UV/vis spectra were consistent with reduction of the benzophenone chromophore, since the typical absorption band at $\lambda_{max} = 254$ nm disappeared. The NMR data collected for the HPLC-separated photoproducts provided unambiguous evidence that they were not the result of hydrogen abstraction from the C2-methine group of the tetrahydrofuran residue, but rather from the C5-methylene group.

As the reaction ensues with formation of two new chiral centers, four diastereomers can theoretically be expected for each conjugate. Fortunately, crystals of sufficient quality for X-ray analysis were obtained for **6aB**, **6aD**, and **6bB**−**6bD** (*cf.* Figure 5). This allowed the determination of the stereochemistry of the photoproducts and confirmed the NMR-anticipated regioselectivity of hydrogen abstraction. It was not possible to obtain high quality crystals of compound **6bA**; nevertheless, its stereochemistry was safely assigned as the X-ray structures (**6bB**−**6bD**) of three out of four possible diastereomers were available.

Noteworthy, no C−C coupling products were obtained upon irradiation of the ketoprofen−alkylbenzene conjugates **3a** and **3b**, which turned out to be considerably photostable. By contrast, photolysis of the analogous conjugates **4a** and **4b** with a longer spacer gave complex mixtures of photoproducts (see structures in Scheme 3), which were analyzed by HPLC (*cf.* Figure 6). In the case of **4a**, photoproducts **7aA** and **7aB** were completely separated by means of a reversed phase column. However, subsequent resolution with a chiral HPLC column was necessary to isolate photoproducts **8A**−**8D**. On the other hand, irradiation of **4b** led to the formation of four products, **7bA**−**7bD** [*cf.* Figure 6 (bottom)], in addition to the other four (**8A**−**8D**), which were also obtained from **4a**. As stated above for photoproducts **6**, UV/vis (no benzophenone absorption) and MS-ES (isobaric [MH^+] peaks, $m/z = 430$) spectra of the photoproducts were consistent with C−C coupling *via* biradical recombination. The NMR data of the isolated products indicated hydrogen abstraction from two different positions of the alkylbenzene moiety, namely the methine (**8A**−**8D**) or the methylene group (**7aA**, **7aB**, and **7bA**−**7bD**).

The stereochemistry of the common photoproducts **8A**−**8D** was safely assigned by X-ray analysis (*cf.* Figure 7), as

Chart 3

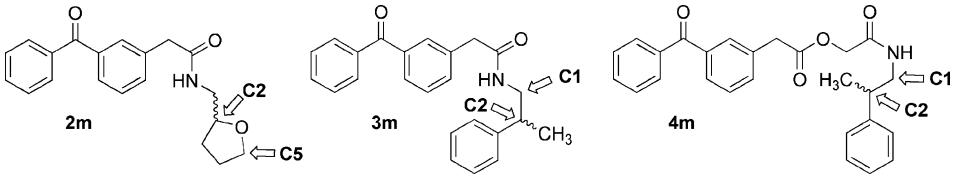

Scheme 4. Energy Level Diagrams for Formation of Biradicals *via* Hydrogen Transfer in **2m**, **3m**, and **4m** (t: Triplet State)[a]

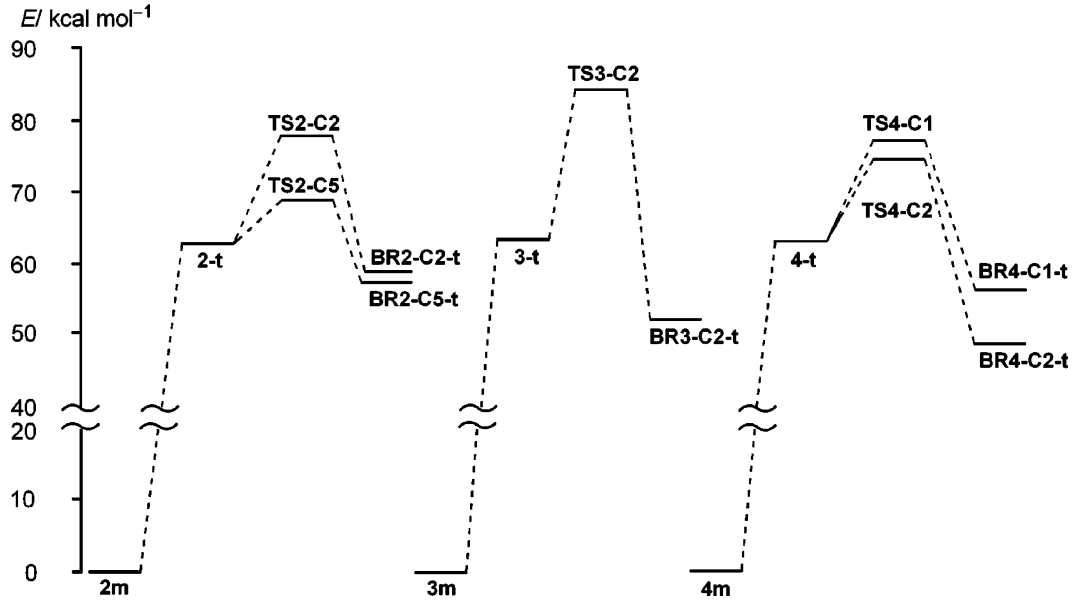

[a] The optimized transition state (TS) and biradical (BR) structures can be found in the Supporting Information.

appropriate crystals of three out of the four possible diastereomers were available. Regarding the other photoproducts, crystal structures were obtained for **7aA** and **7bA**−**7bC**. Thus, the stereochemistry of **7bD** was unambiguously assigned, because only one possibility remained for the fourth isomer. In the case of **7aB** a combination of NOE effects and simple molecular modeling (AM1) was used to determine the configuration of the newly generated asymmetric carbons (*cf.* Supporting Information). Due to the rigidity of the macrocyclic structures, NOE effects are particularly useful. Figure 8 shows Newman projections of the relevant substructures for **7aA**−**7aD**, based on the AM1-optimized structures. Note that, in the case of **7aA**, this structure is essentially co-incident with that established by X-ray diffraction. The most relevant NOE interaction for compounds **7aA** and **7aB** was observed between the *ortho*-protons of the phenyl group of the former benzophenone and the methine hydrogen α-standing to the amido group. Such interaction cannot be expected for **7aC** and **7aD** (not obtained).

Regioselectivity in Hydrogen Transfer and Diastereoselectivity in C−**C Coupling.** The yields of the different photoproducts arising from irradiation of **2a**,**b** and **4a**,**b** are compiled in Table 2. Based on these data, the regio- and stereoselectivity of the photoreaction will be discussed in the following paragraphs. A clear-cut observation is that in the ketoprofen−tetrahydrofuran conjugates (**2a** and **2b**) hydrogen abstraction occurs only from the C5-methylene group, in spite of the lower dissociation energy expected for the C2−H bond due to the higher degree of substitution. In other words, the process is completely regioselective for **2a** and **2b**, which is likely a consequence of the higher strain expected for the cyclic transition state for abstraction from C2−H (see also DFT calculations).

By contrast, for **4a** and **4b**, where the spacer is longer, hydrogen abstraction occurred from two different positions of the donor moiety, namely the methylene (**7aA**, **7aB**, and **7bA**−**7bD**) and the methine group (**8A**−**8D**). Based on thermodynamic arguments, hydrogen abstraction from the benzylic C−H (photoproducts **8**) should be energetically favored. However, formation of photoproducts **7** was always preferred, especially for **4b**, as shown by the **7**/**8** ratio (1.1 for **4a** and 1.7 for **4b**). This emphasizes the prevailing role of the spacer in the cyclic transition state, which overrides thermodynamic arguments. Thus, as for **2a** and **2b**, hydrogen abstraction does not occur selectively from the more substituted carbon.

On the other hand, the data in Table 2 also point to a remarkable stereoselectivity in C−C bond formation from the respective biradicals. For **2a**, photoproducts **6aB** and **6aD**, corresponding to *cisoid* ring junction of the bicyclic system, were exclusively obtained. Conversely, in the case of **2b**, both *cisoid* and *transoid* ring junction products were formed, albeit the former were favored (**A**+**C**/**B**+**D** ratio of 1.6). The observed predominance of *cisoid* products is in agreement with the smaller ring strain associated with macrocyclization.

Likewise, for the ketoprofen−alkylbenzene conjugates **4a** and **4b**, diastereoselectivity was also noted for hydrogen abstraction from the prochiral methylene group. Thus, in the case of **4a** only two stereoisomers (**7aA** and **7aB**) out of the four possible photoproducts were observed. As regards **4b**, all four stereoisomers (**7bA**−**7bD**) were obtained, but with different yields. Concerning the products of hydrogen abstraction from the chiral

Table 3. Crystallographic Data and Structure Refinement Information for **6aB**, **6aD**, **6bB**−**6bD**

	6aB	6aD	6bB	6bC	6bD
formula	$C_{21}H_{23}NO_3$	$C_{21}H_{23}NO_3$	$C_{21}H_{23}NO_3$	$C_{21}H_{23}NO_3$	$C_{21}H_{23}NO_3$
formula weight	337.4	337.4	337.4	337.4	337.4
color	colorless	colorless	colorless	colorless	colorless
crystal system	orthorhombic	monoclinic	triclinic	monoclinic	orthorhombic
space group	*P* 21 21 21	*P* 21	*P* 1	*P* 21	*P* 21 21 21
a (Å)	8.5224 (2)	8.207 (2)	8.460 (5)	7.572 (5)	7.911 (5)
b (Å)	8.8972 (2)	27.329 (7)	10.152 (5)	10.001 (5)	10.919 (5)
c (Å)	22.2197 (5)	15.559 (2)	11.884 (5)	11.441 (5)	20.202 (5)
α (deg)	90	90	71.846 (5)	90 (5)	90 (5)
β (deg)	90	104.792 (10)	83.081 (5)	101.246 (5)	90 (5)
γ (deg)	90	90	71.356 (5)	90 (5)	90 (5)
V (Å^3)	1684.82 (7)	3374.2 (12)	918.7 (8)	849.8 (8)	1745.1 (14)
T (K)	120 (10)	120 (1)	120 (2)	120 (2)	120 (2)
Z	4	8	1	2	4
R	0.0465	0.0765	0.0326	0.0214	0.0297
GOF	1.059	1.064	1.062	1.057	1.067

Table 4. Crystallographic Data and Structure Refinement Information for **7aA**, **7bA**−**7bC**, **8B**−**8D**

	7aA	7bA	7bB	7bC	8B	8C	8D
formula	$C_{27}H_{27}NO_4$	$C_{27}H_{27}NO_4$	$C_{27}H_{27}NO_4$	$C_{27}H_{27}NO_4$	$C_{27}H_{27}NO_4$	$C_{27}H_{27}NO_4$	$C_{27}H_{27}NO_4$
formula weight	429.5	429.5	429.5	429.5	429.5	429.5	429.5
color	colorless	colorless	colorless	colorless	colorless	colorless	colorless
crystal system	monoclinic	tetragonal	monoclinic	monoclinic	triclinic	monoclinic	orthorhombic
space group	*P* 21	*P* 43	*P* 21	*P* 21	*P* 1	*P* 21	*P* 21 21 21
a (Å)	12.3969 (5)	11.4707 (5)	12.3586 (19)	9.359 (3)	6.345 (5)	9.1634 (5)	11.5577 (15)
b (Å)	5.3641 (2)	11.4707 (5)	5.6122 (6)	10.3678 (8)	8.183 (5)	10.9182 (6)	13.9554 (13)
c (Å)	16.9165 (7)	19.7124 (18)	16.2206 (23)	11.941 (2)	11.894 (5)	11.5433 (6)	14.1742 (14)
α (deg)	90	90	90	90	72.862 (5)	90	90
β (deg)	103.524 (2)	90	98.289 (9)	104.583 (16)	84.838 (5)	112.823 (2)	90
γ (deg)	90	90	90	90	68.755 (5)	90	90
V (Å^3)	1093.73 (8)	2593.7 (3)	1113.28 (26)	1121.4 (4)	549.9 (6)	1064.46 (10)	2286.2 (4)
T (K)	293 (2)	100 (2)	293 (2)	293 (2)	273 (2)	100 (2)	
Z	2	4	2	2	1	2	4
R	0.0541	0.0550	0.046	0.1056	0.0270	0.0878	0
GOF	1.128	1.039	1.011	1.079	1.075	0.993	1.19

benzylic position (**8A**−**8D**), the distribution did not depend on the configuration of the starting compound; no stereoselectivity was observed.

DFT Calculations. In order to rationalize the experimental observations, DFT calculations, using B3LYP exchange-correlation functionals together with the standard 6-31G* basis set, were carried out (see Experimental Section). The compounds **2m**, **3m**, and **4m** were introduced as models; they are closely related to the experimentally investigated systems but lack the methyl group adjacent to the benzophenone. This allowed us to draw conclusions about the influence of the spacer and hydrogen donor on the photoreactivity and the regioselectivity, avoiding interferences due to diastereodifferentiation.

Scheme 4 shows simplified energy level diagrams for intramolecular hydrogen abstractions in **2m**−**4m** (for a comprehensive data set of energies, see Table 2 in the Supporting Information). Different possibilities for the regioselectivity (see marked positions in Chart 3) were taken into account. In the case of **3m** only hydrogen abstraction from the benzylic methine C2 was considered. Involvement of the methylene C1 would give rise to a highly strained, and therefore unlikely, transition state, similar to the situation encountered for C2 in **2m** (see below).

A closer inspection of Scheme 4 leads to several immediate observations: (*a*) all conjugates have (gas-phase) triplet state excitation energies of *ca.* 63 kcal mol^{-1}, which is in reasonable agreement with the value for parent benzophenone in nonpolar solvents (*ca.* 69 kcal mol^{-1}).[74] (*b*) Hydrogen abstraction in **2m** shows a strong preference for the C5 position. The activation energy E_a for this channel is 6.2 kcal mol^{-1}, which is 8.8 kcal mol^{-1} lower than that calculated for the C2 position. This is in excellent agreement with the experimentally observed regioselectivity for **2a** and **2b** (see above). (*c*) For **4m** only a small difference in the activation energies for abstraction from C1 or C2 was calculated [$\Delta E_a = 2$ kcal mol^{-1} with E_a(C1) > E_a(C2)]. Noteworthy, also experimentally less pronounced regioselectivity was observed for **4a** and **4b**. (*d*) The calculated activation energies for the most favorable hydrogen abstraction pathway [E_a(**2m**) < E_a(**4m**) < E_a(**3m**)] fully support the experimentally observed reactivity order (*cf.* Table 1). In conclusion, DFT calculations on the model compounds confirmed the experimental observations related to reactivity and regioselectivity in the initial hydrogen transfer step.

(74) Murov, S. L.; Carmichael, I.; Hug, G. L. *Handbook of Photochemistry*, 2nd ed.; Marcel Dekker, Inc.: New York, 1993.

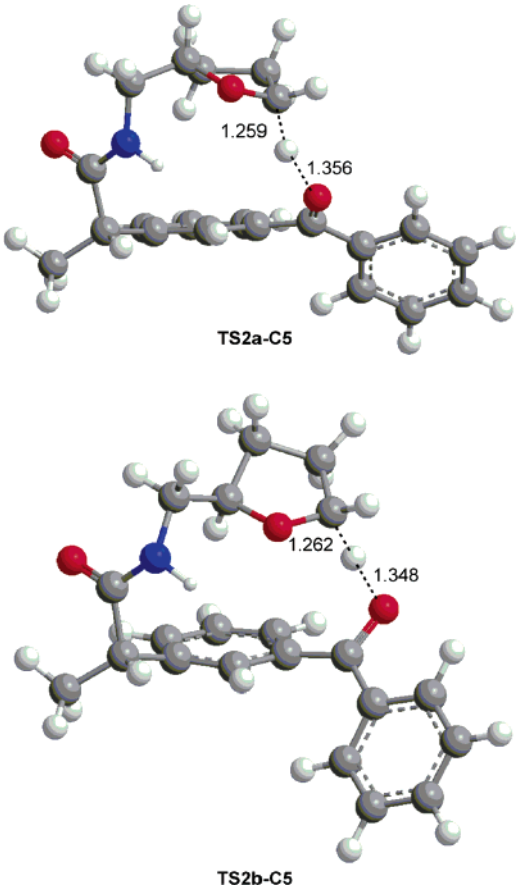

Figure 9. Transition state structures for the intramolecular hydrogen abstraction from C5 in **2a** (top) and **2b** (bottom). The numbers indicate the respective O−H and C−H bond lengths (in Å).

The compounds **2a** and **2b** showed the largest diastereodifferentiation for hydrogen transfer among the investigated systems. Therefore, we attempted to reproduce the observed stereoselectivity trend with DFT calculations. The optimized geometries of the transition states for hydrogen abstraction from the favored C5 position are shown in Figure 9. Based on the energies of the excited triplet state and transition state found for each diastereomer (see Table 3 in the Supporting Information), the obtained activation barriers were 9.9 kcal mol^{-1} and 14.5 kcal mol^{-1} for **2a** and **2b**, respectively. Thus, the activation energies agree well with the higher reactivity of **2a** as compared to **2b**.[75] As the formed biradicals have about the same energy (*ca.* 5 kcal mol^{-1} below the excited triplet state of the reactant), the differences in the transition state energies are likely the result of ring strain effects and steric constraints.

Conclusions

Diastereomeric conjugates, which are composed of a benzophenone chromophore and tetrahydrofuran or isopropylbenzene moieties as hydrogen donors, were synthesized, and their photophysical and photochemical behavior was investigated. The kinetics of the initial hydrogen transfer step (k_H *ca.* 10^4-10^5 s^{-1}) is significantly dependent on the inherent chiral information contained in the conjugates. Thus, an interesting diastereodifferentiation has been noted for **2a** and **2b**, which is manifested in triplet lifetimes of 1.6 and 2.7 μs, respectively. Differentiations were also observed for **3a**,**b** while being absent for **4a**,**b**. The general order of reactivity [k_H(**2a**,**b**) > k_H(**4a**,**b**) > k_H(**3a**,**b**)] was confirmed by DFT calculations with model compounds (**2m**−**4m**), which yielded the lowest activation energy for triplet biradical formation from **2m** and the highest for **3m**. For the example of the most pronounced diastereodifferentiation (**2a** and **2b**) further calculations revealed an activation energy difference of 4.6 kcal mol^{-1}, thereby confirming the observed faster decay kinetics for excited triplet **2a**. For the example of intermolecular quenching of (*S*)-ketoprofen **1** by tetrahydrofuran derivatives **5a** and **5b** a remarkable enantiodifferentiation was evidenced as well.

The remote hydrogen transfer yields biradicals, which decay by intramolecular recombination. Transient absorption spectra show only the benzophenone-like triplet−triplet absorptions but no signals for the biradicals. This points to a short lifetime of these intermediates, which do therefore not accumulate. The resulting fast recombination leads to macrocyclic photoproducts, which contain one or two additional asymmetric carbon centers. The overall photoreaction quantum yields parallel the reactivity trends noted for the initial step of the mechanism. All formed photoproducts were isolated and extensively characterized (^{1}H and ^{13}C NMR, NOE, single-crystal X-ray), which allows us to draw conclusions about the regio- and stereoselectivity of the cyclization reaction. The compounds **2a** and **2b** show only hydrogen abstraction from the less substituted C5 position of the tetrahydrofuran ring (photoproducts **6**). Hydrogen abstraction from C2 was not observed, because of the ring strain of the associated cyclic transition state. DFT calculations confirmed this qualitative argument and revealed that the activation energy for the pathway involving C5 is 8.8 kcal mol^{-1} lower than that for C2. With respect to the configuration of the newly formed asymmetric centers, a preferred *cisoid* ring junction is observed. **3a** and **3b** show almost no photoreaction (Φ_r < 0.05), while **4a** and **4b**, with an elongated spacer, form photoproducts. Products of hydrogen abstraction from the methylene α-standing to the amide *N* (**7**) or the chiral methine (**8**) were almost equally distributed in the case of **4a**, while the former were favored for **4b**. However, in comparison to **2a** and **2b**, the regioselectivity of cyclization was not absolute, which might be traced back to the more flexible spacer in **4a** and **4b**. These experimental results were corroborated by DFT calculations with **4m**, which yielded low and comparable activation energies for both pathways.

In summary, remote hydrogen abstraction reactions in diastereomeric conjugates composed of ketoprofen and quencher moieties, which might serve as photobiological model systems, have been comprehensively investigated at two levels: the initial hydrogen transfer step and the intramolecular recombination of the formed biradicals to macrocyclic photoproducts. Our results show that diastereodifferentiation in excited-state hydrogen transfer is indeed an important feature, which might lead to pronounced reactivity tuning. Given that ketoprofen is an essential part of our compounds, implications for differentiated photoinduced effects of the enantiomeric forms of this drug in real supramolecular complexes with bioactive structures like DNA or peptides might apply.

Experimental Section

Materials. All chemicals required for the synthesis of the ketoprofen−quencher conjugates were purchased from Aldrich. *n*-Hexane,

(75) However, the significance of the absolute numerical values for the activation energies should not be overemphasized because of the inherent errors of the calculation method (ca. 1 kcal mol^{-1}).

acetonitrile, methanol, and ethanol, which were used for photophysical measurements and/or analytical and semipreparative chromatography, were of HPLC quality from Merck. Silica gel (230−400 mesh) from Scharlau was used for column chromatography. Ethyl acetate, *n*-hexane, and dichloromethane from Scharlau were used for flash chromatography.

Measurements. All spectroscopic measurements were done at room temperature (296 K) with nitrogen-purged acetonitrile solutions, using quartz cuvettes of 1 cm optical path length. UV/vis-absorption spectra were recorded with a Shimadzu UV-2101 spectrometer. Steady-state-photolysis of optically matched solutions ($A = 1.5$) of the conjugates at $\lambda_{exc} = 254$ nm at an analytical scale was carried out within a Photon Technology International (PTI) LPS-220B fluorimeter. Quantum yields were determined using phenylglyoxylic acid as actinometer.[76]

Laser flash photolysis studies were done with a homemade setup using a Nd:YAG laser ($\lambda_{exc} = 266$ nm, *ca.* 10 ns pulse width, 10 mJ/pulse) as the excitation source. A pulsed Lo255 Oriel xenon lamp served for the generation of the analyzing light beam. The observation wavelength was selected with a 77200 Oriel monochromator, and the signal was amplified by an Oriel photomultiplier tube (PMT) system made up of a 77348 side-on PMT tube, a 70680 PMT housing, and a 70705 PMT power supply. The signal was registered with a TDS-640A Tektronix oscilloscope and subsequently transferred to a personal computer. The applied excitation wavelength ($\lambda_{exc} = 266$ nm) allowed us to work with highly diluted solutions of the conjugates (10^{-5} M), thus, minimizing self-quenching. This offered the possibility to study the kinetics of triplet quenching in a wider dynamic range as compared to $\lambda_{exc} = 355$ nm.

HPLC analysis was performed using either a Varian HPLC system equipped with a polychrome diode array detector (Varian 9065) or a 1100 Series MSD Agilent instrument with an API-ES positive ionization mode for mass detection. Product yields (*cf.* Table 2) are based on HPLC measurements by using isolated photoproducts as standards. NMR measurements were done with a Bruker 300 spectrometer at 296 K.

Computational Methods. DFT calculations were carried out using the B3LYP[77,78] exchange-correlation functionals, together with the standard 6-31G* basis set.[79] The unrestricted formalism (UB3LYP) was employed for all calculations. Optimizations were achieved by using the Berny analytical gradient method.[80,81] Stationary points were characterized by frequency calculations, in order to verify that the transition state (TS) structures have only one imaginary frequency. The intrinsic reaction coordinate (IRC)[82] path was traced in order to check the energy profiles connecting each TS with the two associated minima (excited triplet state and biradical) of the proposed mechanism by using the second-order González−Schlegel integration method.[83,84] All calculations were carried out with the Gaussian 03 program package.[85]

Preparation of 2a and 2b. The synthesis was performed by condensation of (*S*)-ketoprofen (0.8 mmol) with (*S*)- or (*R*)-(tetrahydrofuran-2-yl)methylamine (1.0 mmol) in dry dichloromethane (10 mL), using 1-ethyl-3-(3-dimethylamino)propylcarbodiimide (EDC, 1.0 mmol) for activation of the acid. The mixture was stirred at room temperature overnight. After standard aqueous workup, the compounds were purified by flash chromatography on silica gel using ethyl acetate/*n*-hexane (4/1 v/v) as eluent, obtaining **2a** or **2b** as a colorless solid or oil, respectively.

2-(3-Benzoylphenyl)-*N*-[(2*S*)-tetrahydrofuran-2-yl]methyl)-(2*S*)-propionamide (2a). ^{1}H NMR (300 MHz, $CDCl_3$): δ 7.81−7.71 (m, 3H), 7.68−7.62 (m, 1H), 7.61−7.54 (m, 2H), 7.51−7.38 (m, 3H), 5.89 (br. s, 1H), 3.95−3.85 (m, 1H), 3.70−3.56 (m, 3H), 3.55−3.45 (m, 1H), 3.17−3.07 (m, 1H), 1.92−1.63 (m, 3H), 1.53 (d, $J = 7.2$ Hz, 3H), 1.45−1.31 (m, 1H). ^{13}C NMR (75 MHz, $CDCl_3$): δ 196.5, 173.5, 142.0, 138.0, 137.5, 132.5, 131.5, 130.0, 129.1, 129.0, 128.7, 128.3, 77.7, 68.1, 47.0, 43.0, 28.4, 25.8, 18.6. HRMS (EI): calcd for $C_{21}H_{23}NO_3$, 337.1678; found, 337.1637.

2-(3-Benzoylphenyl)-*N*-[(2*R*)-tetrahydrofuran-2-yl]methyl)-(2*S*)-propionamide (2b). ^{1}H NMR (300 MHz, $CDCl_3$): δ 7.82−7.72 (m, 3H), 7.70−7.64 (m, 1H), 7.63−7.55 (m, 2H), 7.52−7.42 (m, 3H), 5.77 (br. s, 1H), 3.92−3.82 (m, 1H), 3.80−3.58 (m, 3H), 3.55−3.45 (m, 1H), 3.22−3.11 (m, 1H), 1.96−1.78 (m, 4H), 1.55 (d, $J = 7.4$ Hz, 3H). ^{13}C NMR (75 MHz, $CDCl_3$): δ 196.5, 173.7, 141.7, 138.1, 137.5, 132.5, 131.5, 130.1, 129.2, 129.1, 128.8, 128.3, 77.6, 68.1, 47.1, 43.2, 28.5, 25.9, 18.7. HRMS (EI): calcd for $C_{21}H_{23}NO_3$, 337.1678; found, 337.1673.

Preparation of 3a and 3b. The synthesis was performed by reaction of (*S*)-ketoprofen (0.8 mmol) with (*S*)- or (*R*)-2-phenylpropylamine (1 mmol) in dry dichloromethane (10 mL) in the presence of EDC (1 mmol). After extraction with water the organic phase was dried, and the obtained crude mixture was purified by silica gel flash chromatography using ethyl acetate/*n*-hexane (4/1 v/v) as eluent. Both **3a** and **3b** were obtained as colorless oils.

2-(3-Benzoylphenyl)-*N*-[(2*S*)-phenylethyl]methyl)-(2*S*)-propionamide (3a). ^{1}H NMR (300 MHz, $CDCl_3$): δ 7.80−7.74 (m, 2H), 7.69−7.57 (m, 3H), 7.53−7.37 (m, 4H), 7.24−7.11 (m, 3H), 7.02−6.96 (m, 2H), 5.19 (br. s, 1H), 3.67−3.56 (m, 1H), 3.48 (q, $J = 7.2$ Hz, 1H), 3.16−3.05 (m, 1H), 2.89−2.74 (m, 1H), 1.48 (d, $J = 7.2$ Hz, 3H), 1.20 (d, $J = 6.9$ Hz, 3H). ^{13}C NMR (75 MHz, $CDCl_3$): δ 196.3, 173.3, 143.7, 141.7, 138.0, 137.4, 132.5, 131.4, 130.0, 129.1, 129.0, 128.7, 128.6, 128.3, 127.1, 126.7, 47.0, 46.2, 39.6, 19.0, 18.4. HRMS (EI) calcd for $C_{25}H_{25}NO_2$: 371.1885; found: 371.1890.

2-(3-Benzoylphenyl)-*N*-[(2*R*)-phenylethyl]methyl)-(2*S*)-propionamide (3b). ^{1}H NMR (300 MHz, $CDCl_3$): δ 7.80−7.74 (m, 2H), 7.67−7.57 (m, 3H), 7.53−7.35 (m, 4H), 7.28−7.13 (m, 3H), 7.08−7.02 (m, 2H), 5.18 (br. s, 1H), 3.56−3.46 (m, 2H), 3.29−3.18 (m, 1H), 2.94−2.81 (m, 1H), 1.48 (d, $J = 7.2$ Hz, 3H), 1.19 (d, $J = 7.0$ Hz, 3H). ^{13}C NMR (75 MHz, $CDCl_3$): δ 196.4, 173.3, 143.7, 141.6, 138.0, 137.4, 132.5, 131.5, 130.0, 129.0, 128.7, 128.6, 128.3, 127.1, 126.7, 47.0, 46.1, 39.6, 19.0, 18.4. HRMS (EI): calcd for $C_{25}H_{25}NO_2$, 371.1885; found, 371.1853.

Preparation of 4a and 4b. To a solution of (*S*)-ketoprofen (2.4 mmol) in ethyl acetate (8 mL) triethylamine (2.4 mmol) was slowly added. After 30 min, phenyl bromoacetate (2.8 mmol) was added, and the reaction mixture was stirred for 48 h. Thereafter, the organic phase was washed with water, and the crude product was isolated by evaporation of the solvent. The obtained phenyl ester (1.0 mmol) was reacted with (*S*)- or (*R*)-2-phenylpropylamine (1.2 mmol) in dry dichloromethane (12 mL). After standard workup, the products were purified by flash chromatography on silica gel using ethyl acetate/*n*-hexane (1/1 v/v) as eluent, affording colorless oils.

(2*S*)-(3-Benzoylphenyl)propanoyloxy-*N*-[(2*S*)-phenylpropyl]acetamide (4a). ^{1}H NMR (300 MHz, $CDCl_3$): δ 7.83−7.77 (m, 2H), 7.73−7.58 (m, 3H), 7.54−7.35 (m, 4H), 7.35−7.19 (m, 3H), 7.18−7.11 (m, 2H), 5.66 (br. s, 1H), 4.56 (d, $J = 15.5$ Hz, 1H), 4.45 (d, $J = 15.5$ Hz, 1H), 3.73 (q, $J = 7.2$ Hz, 1H), 3.61−3.50 (m, 1H), 3.27−3.16 (m, 1H), 2.90−2.75 (m, 1H), 1.47 (d, $J = 7.2$ Hz, 3H), 1.20 (d, $J = 6.9$ Hz, 3H). ^{13}C NMR (75 MHz, $CDCl_3$): δ 196.1, 172.2, 166.6, 143.6, 140.1, 138.2, 137.3, 132.6, 131.1, 130.0, 129.3, 129.0, 128.8, 128.4, 127.1, 126.9, 63.1, 45.5, 45.2, 39.5, 19.1, 18.2. HRMS (EI): calcd for $C_{27}H_{27}NO_4$, 429.1940; found, 429.1951.

(76) Kuhn, H. J.; Defoin, A. *EPA Newslett.* **1986**, *26*, 23−25.
(77) Lee, C. T.; Yang, W. T.; Parr, R. G. *Phys. Rev. B* **1988**, *37*, 785−789.
(78) Becke, A. D. *J. Chem. Phys.* **1993**, *98*, 5648−5652.
(79) Hehre, W. J.; Radom, L.; Schleyer, P. v. R.; Pople, J. A. *Ab initio Molecular Orbital Theory*; Wiley: New York 1986.
(80) Schlegel, H. B. *J. Comput. Chem.* **1982**, *3*, 214−218.
(81) Schlegel, H. B. Geometry Optimization on Potential Energy Surfaces. In *Modern Electronic Structure Theory*; Yarkony, D. R., Ed.; World Scientific Publishing: Singapore, 1995; pp 459−500.
(82) Fukui, K. *J. Phys. Chem.* **1970**, *74*, 4161−4163.
(83) Gonzalez, C.; Schlegel, H. B. *J. Phys. Chem.* **1990**, *94*, 5523−5527.
(84) Gonzalez, C.; Schlegel, H. B. *J. Chem. Phys.* **1991**, *95*, 5853−5860.
(85) Frisch, M. J., et al. *Gaussian 03*, revision C.02; Gaussian, Inc.: Wallingford, CT, 2004.

(2*S*)-(3-Benzoylphenyl)propanoyloxy-*N*-[(2*R*)-phenylpropyl]acetamide (4b). ^{1}H NMR (300 MHz, $CDCl_3$): δ 7.82−7.76 (m, 2H), 7.72−7.58 (m, 3H), 7.54−7.45 (m, 2H), 7.45−7.37 (m, 2H), 7.34−7.19 (m, 3H), 7.18−7.11 (m, 2H), 5.68 (br. s, 1H), 4.50 (s, 2H), 3.71 (q, J = 7.2 Hz, 1H), 3.68−3.56 (m, 1H), 3.21−3.09 (m, 1H), 2.91−2.78 (m, 1H), 1.47 (d, J = 7.2 Hz, 3H), 1.20 (d, J = 7.2 Hz, 3H). ^{13}C NMR (75 MHz, $CDCl_3$): δ 196.2, 172.2, 166.6, 143.6, 140.1, 138.2, 137.3, 132.7, 131.2, 130.1, 129.3, 128.9, 128.8, 128.7, 128.4, 127.1, 126.9, 63.1, 45.5, 45.1, 39.6, 19.1, 18.0. HRMS (EI): calcd for $C_{27}H_{27}NO_4$, 429.1940; found, 429.1945.

Preparation of Enantiomeric Acetamides 5a and 5b. The synthesis was accomplished by reacting (*S*)- or (*R*)-(tetrahydrofuran-2-yl)-methylamine (1.0 mmol) with a slight excess of acetyl chloride (1.1 mmol) in the presence of triethylamine (1.2 mmol) in 10 mL of dry dichloromethane. After standard aqueous workup, the products were purified by column chromatography (silica gel and ethyl acetate/methanol 1/1 v/v as eluent) and subsequent vacuum distillation (130 °C, 5 mmHg). The products were obtained as colorless oils.

***N*-[(2*S*)-(Tetrahydrofuran-2-yl)methyl]acetamide (5a) and *N*-[2-(*R*)-(Tetrahydrofuran-2-yl)methyl]acetamide (5b).** ^{1}H NMR (300 MHz, $CDCl_3$): δ 5.94 (br. s, 1H), 3.99−3.88 (m, 1H), 3.88−3.69 (m, 2H), 3.62−3.52 (m, 1H), 3.12−3.01 (m, 1H), 2.03−1.81 (m, 4H), 1.97 (s, 3H). ^{13}C NMR (75 MHz, $CDCl_3$): δ 173.5, 77.7, 68.0, 43.3, 28.6, 25.8, 23.2. HRMS (EI): calcd for $C_7H_{14}NO_2$ (MH) (**5a**), 144.1025; found, 144.1016. HRMS (EI): calcd for $C_7H_{14}NO_2$ (MH) (**5b**), 144.1025; found, 144.1019.

General Procedure for Preparative Irradiation of the Ketoprofen−Quencher Conjugates. The compounds were irradiated at room temperature with a Rayonet photoreactor equipped with 12 lamps (8 W, λ_{max} = 350 nm) in pyrex flasks. The substrates (2 mmol) were dissolved in acetonitrile (1 L) and degassed for 30 min with a continuous stream of nitrogen. The solutions were irradiated until the reaction was completed as monitored by HPLC/UV/MS analysis. After evaporation of the solvent, the residue was subjected to semipreparative HPLC.

Isolation of Photoproducts 6aB and 6aD. The crude mixture obtained by irradiation of **2a** was submitted to semipreparative HPLC (Kromasil 100, reversed phase C18, 5 μm, length 25 cm, diameter 1.0 cm) using water/acetonitrile/methanol (40/30/30 v/v/v) as eluent. The system was operated under isocratic conditions at a flow rate of 4 mL min^{-1}. Two major photoproducts (**6aB** and **6aD**) were isolated and characterized.

2-Hydroxy-8-methyl-9-oxo-2-phenyl-(1*R*,2*R*,8*S*,12*S*)-15-oxa-10-azatricyclo[10.2.1.1^{3,7}]hexadeca-3,5,7(16)-triene (6aB). ^{1}H NMR (300 MHz, $CDCl_3$): δ 7.78−7.73 (m, 1H), 7.71−7.66 (m, 2H), 7.45−7.21 (m, 5H), 7.10 (s, 1H), 5.36 (br. s, 1H), 4.76 (dd, J = 9.4 Hz, 2.6 Hz, 1H), 3.86−3.77 (m, 1H), 3.59 (q, J = 7.2 Hz, 1H), 3.55−3.44 (m, 1H), 3.42−3.31 (m, 1H), 1.95−1.84 (m, 1H), 1.81−1.70 (m, 1H), 1.50 (d, J = 7.2 Hz, 3H), 1.20−1.08 (m, 1H), −0.57 (m, 1H). ^{13}C NMR (75 MHz, $CDCl_3$): δ 176.3, 145.5, 140.2, 138.4, 133.0, 128.6, 128.3, 128.1, 127.9, 124.4, 123.0, 81.7, 80.8, 79.9, 47.0, 39.4, 27.0, 26.7, 11.7. HRMS (EI): calcd for $C_{21}H_{23}NO_3$, 337.1678; found, 337.1670.

2-Hydroxy-8-methyl-9-oxo-2-phenyl-(1*R*,2*S*,8*S*,12*S*)-15-oxa-10-azatricyclo[10.2.1.1^{3,7}]hexadeca-3,5,7(16)-triene (6aD). ^{1}H NMR (300 MHz, $CDCl_3$): δ 8.07 (s, 1H), 7.46−7.33 (m, 5H), 7.24−7.22 (m, 1H), 7.13 (t, J = 7.6 Hz, 1H), 6.47−6.42 (m, 1H), 5.78 (br. s, 1H), 4.74 (dd, J = 9.7 Hz, 2.7 Hz, 1H), 3.86 (q, J = 7.2 Hz, 1H), 3.82−3.74 (m, 1H), 3.65−3.54 (m, 1H), 3.48−3.39 (m, 1H), 2.12−1.96 (m, 1H), 1.58 (d, J = 7.2 Hz, 3H), 1.54−1.44 (m, 1H), 1.24−1.13 (m, 1H), −0.64 (m, 1H). ^{13}C NMR (75 MHz, $CDCl_3$): δ 176.3, 143.2, 140.2, 139.3, 132.3, 128.5, 128.1, 127.6, 127.4, 126.5, 123.4, 82.6, 80.7, 79.8, 47.5, 39.3, 29.1, 26.8, 11.7. HRMS (EI): calcd for $C_{21}H_{23}NO_3$, 337.1678; found, 337.1686.

Isolation of Photoproducts 6bA−6bD. The irradiation mixture from **2b** was resolved by semipreparative HPLC (Kromasil 100, reversed phase C18, 5 μm, length 25 cm, diameter 1.0 cm) using an isocratic mixture of water/methanol (50/50 v/v) as eluent at a flow rate of 4 mL min^{-1}. Thereby the compounds **6bA−6bD** were isolated and subsequently characterized.

2-Hydroxy-8-methyl-9-oxo-2-phenyl-(1*S*,2*S*,8*S*,12*R*)-15-oxa-10-azatricyclo[10.2.1.1^{3,7}]hexadeca-3,5,7(16)-triene (6bA). ^{1}H NMR (300 MHz, $CDCl_3$): δ 7.76−7.71 (m, 1H), 7.65−7.59 (m, 2H), 7.37−7.24 (m, 4H), 7.17−7.11(m, 1H), 6.94 (s, 1H), 4.71 (dd, J = 9.0 Hz, 3.3 Hz, 1H), 4.56 (d, J = 9.0 Hz, 1H), 4.25−4.12 (m, 1H), 3.96−3.86 (m, 1H), 3.42 (q, J = 7.0 Hz, 1H), 2.81−2.72 (d, J = 15.5 Hz, 1H), 2.19 (s, 1H), 2.05−1.91 (m, 1H), 1.87−1.74 (m, 1H), 1.35 (d, J = 7.0 Hz, 3H), 1.31−1.21 (m, 1H), −0.19 (m, 1H). ^{13}C NMR (75 MHz, $CDCl_3$): δ 177.3, 145.8, 141.5, 141.3, 132.2, 128.5, 127.9, 127.8, 127.1, 126.6, 123.7, 81.4, 80.2, 79.4, 47.6, 39.8, 26.5, 25.3, 17.1. HRMS (EI): calcd for $C_{21}H_{23}NO_3$, 337.1678; found, 337.1678.

2-Hydroxy-8-methyl-9-oxo-2-phenyl-(1*R*,2*R*,8*S*,12*R*)-15-oxa-10-azatricyclo[10.2.1.1^{3,7}]hexadeca-3,5,7(16)-triene (6bB). ^{1}H NMR (300 MHz, $CDCl_3$): δ 7.75−7.67 (m, 3H), 7.45−7.06 (m, 5H), 7.00 (s, 1H), 5.49 (s, 1H), 4.86−4.71 (m, 1H), 3.68−3.54 (m, 1H), 3.41 (q, J = 7.0 Hz, 1H), 2.72−2.58 (m, 1H), 2.16−2.02 (m, 1H), 1.52 (d, J = 7.0 Hz, 3H), 1.45−0.97 (m, 4H). ^{13}C NMR (75 MHz, $CDCl_3$): δ 178.1, 147.2, 139.9, 138.3, 132.2, 128.6, 128.1, 127.9, 127.1, 124.1, 79.9, 79.1, 77.2, 49.4, 44.8, 28.5, 28.3, 12.2. HRMS (EI): calcd for $C_{21}H_{23}NO_3$, 337.1678; found, 337.1678.

2-Hydroxy-8-methyl-9-oxo-2-phenyl-(1*S*,2*R*,8*S*,12*R*)-15-oxa-10-azatricyclo[10.2.1.1^{3,7}]hexadeca-3,5,7(16)-triene (6bC). ^{1}H NMR (300 MHz, $CDCl_3$): δ 7.87 (s, 1H), 7.49−7.30 (m, 5H), 7.21−7.02 (m, 2H), 6.52−6.46 (m, 1H), 4.83 (d, J = 9.5 Hz, 1H), 4.72 (dd, J = 9.5 Hz, 3.7 Hz, 1H), 4.29−4.15 (m, 1H), 3.92−3.81 (m, 1H), 3.72 (s, 1H), 3.55 (q, J = 7.0 Hz, 1H), 2.95−2.85 (m, 1H), 2.22−2.06 (m, 1H), 1.62 (d, 3H, J = 7.0 Hz), 1.59−1.47 (m, 1H), 1.39−1.27 (m, 1H), −0.36 (m, 1H). ^{13}C NMR (75 MHz, $CDCl_3$): δ 177.3, 142.7, 142.1, 141.4, 131.6, 128.3, 128.0, 127.7, 127.0, 126.7, 126.1, 82.1, 80.8, 79.2, 48.3, 39.5, 28.7, 25.7, 16.7. HRMS (EI): calcd for $C_{21}H_{23}NO_3$, 337.1678; found, 337.1674.

2-Hydroxy-8-methyl-9-oxo-2-phenyl-(1*R*,2*S*,8*S*,12*R*)-15-oxa-10-azatricyclo[10.2.1.1^{3,7}]hexadeca-3,5,7(16)-triene (6bD). ^{1}H NMR (300 MHz, $CDCl_3$): δ 8.16 (s, 1H), 7.57−7.51 (m, 2H), 7.47−7.34 (m, 4H), 7.17 (t, J = 7.6 Hz, 1H), 6.79 (d, J = 7.6 Hz, 1H), 5.80 (d, J = 10.7 Hz, 1H), 4.81−4.73 (m, 1H), 3.70 (q, J = 6.8 Hz, 1H), 3.65−3.54 (m, 1H), 2.75−2.63 (m, 2H), 2.40−2.29 (m, 1H), 1.65 (d, J = 6.8 Hz, 3H), 1.38−1.18 (m, 3H). ^{13}C NMR (75 MHz, $CDCl_3$): δ 178.2, 142.3, 139.5, 139.0, 133.4, 128.8, 128.4, 128.1, 127.6, 127.5, 125.0, 82.9, 81.7, 79.1, 50.0, 45.3, 30.7, 28.9, 12.0. HRMS (EI): calcd for $C_{21}H_{23}NO_3$, 337.1678; found, 337.1639.

Isolation of Photoproducts 7aA and 7aB. The crude product mixture obtained by irradiation of **4a** was resolved by semipreparative HPLC (Waters Spherisorb ODS2, reversed phase C18, 5 μm, length 25 cm, diameter 2.0 cm) using acetonitrile/water (50/50 v/v) as isocratic solvent, pumped with a flow rate of 10 mL min^{-1}. Two pure photoproducts (**7aA** and **7aB**) as well as a mixed fraction composed by photoproducts **8A−8D** (*cf.* isolation of photoproducts **8A−8D**) were obtained.

2-Hydroxy-9-methyl-5,8-dioxo-2-phenyl-3-[(2*S*)-phenylethyl]-(2*S*,3*S*,9*S*)-7-oxa-4-azabicyclo[8.3.1]tetradeca-1(14),10,12-triene (7aA). ^{1}H NMR (300 MHz, $CDCl_3$): δ 7.75 (s, 1H), 7.56 (d, J = 7.5 Hz, 2H), 7.49 (dd, J = 7.5 Hz, 7.5 Hz, 2H), 7.39 (t, J = 7.5 Hz, 1H), 7.30−7.25 (m, 3H), 7.12 (d, J = 7.8 Hz, 1H), 7.08 (t, J = 7.8 Hz, 1H), 6.96−6.80 (m, 2H), 6.74 (d, J = 7.8 Hz, 1H), 6.18 (d, J = 9.8 Hz, 1H), 4.94 (d, J = 12.6 Hz, 1H), 4.37 (dd, J = 9.8 Hz, 2.5 Hz, 1H), 4.27 (d, J = 12.6 Hz, 1H), 3.82 (q, J = 7.0 Hz, 1H), 3.45−3.34 (m, 1H), 1.51 (d, J = 7.0 Hz, 3H), 1.21 (d, J = 7.2 Hz, 3H). ^{13}C NMR (75 MHz, $CDCl_3$): δ 173.5, 166.4, 142.5, 142.4, 141.6, 136.8, 130.1, 129.4, 128.7, 128.4, 128.2, 127.9, 127.7, 126.8, 124.7, 123.5, 81.7, 65.8, 60.7, 45.9, 39.7, 20.4, 11.8. HRMS (EI): calcd for $C_{27}H_{27}NO_4$, 429.1940; found, 429.1926.

2-Hydroxy-9-methyl-5,8-dioxo-2-phenyl-3-[(2*S*)-phenylethyl]-(2*R*,3*R*,9*S*)-7-oxa-4-azabicyclo[8.3.1]tetradeca-1(14),10,12-triene (7aB).

^{1}H NMR (300 MHz, $CDCl_3$): δ 7.76 (d, J = 7.8 Hz, 2H), 7.52−7.39 (m, 3H), 7.30 (s, 1H), 7.14−7.03 (m, 4H), 6.98 (t, J = 7.5 Hz, 1H), 6.92 (d, J = 7.5 Hz, 2H), 6.76−6.69 (m, 2H), 5.35 (d, J = 14.7 Hz, 1H), 4.88 (dd, J = 10.6 Hz, 5.3 Hz, 1H), 4.76 (d, J = 10.6 Hz, 1H), 4.01 (d, J = 14.7 Hz, 1H), 3.69 (q, J = 7.0 Hz, 1H), 3.07−2.96 (m, 1H), 2.40 (br s, 1H), 1.56 (d, J = 7.0 Hz, 3H), 1.16 (d, J = 7.2 Hz, 3H). ^{13}C NMR (75 MHz, $CDCl_3$): δ 173.7, 166.7, 142.8, 141.5, 139.2, 138.4, 129.0, 128.9, 128.6, 128.3, 128.1, 127.4, 126.6, 126.3, 126.0, 124.8, 83.4, 63.5, 62.1, 46.5, 41.4, 23.3, 16.9. HRMS (EI): calcd for $C_{27}H_{27}NO_4$, 429.1940; found, 429.1930.

Isolation of Photoproducts 7bA−7bD. The irradiation mixture obtained from **4b** was dissolved in acetonitrile and injected into a semipreparative HPLC system (Waters Spherisorb ODS2, reversed phase C18, 5 μm, length 25 cm, diameter 2.0 cm) using acetonitrile/water (50/50 v/v) as isocratic eluent. The system was operated at a flow rate of 10 mL min^{-1}. Photoproducts **7bA−7bD** were isolated and characterized as pure compounds. An additional mixed fraction including compounds **8A−8D** was also obtained (*cf.* isolation of photoproducts **8A−8D**).

2-Hydroxy-9-methyl-5,8-dioxo-2-phenyl-3-[(2*R*)-phenylethyl]-(2*S*,3*S*,9*S*)-7-oxa-4-azabicyclo[8.3.1]tetradeca-1(14),10,12-triene (7bA). ^{1}H NMR (300 MHz, $CDCl_3$): δ 7.87−7.70 (m, 4H), 7.63 (d, J = 8.0 Hz, 1H), 7.52−7.38 (m, 5H), 7.18−7.07 (m, 3H), 6.87−6.70 (m, 1H), 4.95 (d, J = 10.0 Hz, 1H), 4.63 (d, J = 13.2 Hz, 1H), 4.62 (m, 1H), 4.42 (d, J = 13.2 Hz, 1H), 3.95 (q, J = 7.2 Hz, 1H), 3.23−3.12 (m, 1H), 1.46 (d, J = 7.2 Hz, 3H), 1.24 (d, J = 7.2 Hz, 3H). ^{13}C NMR (75 MHz, $CDCl_3$): δ 174.5, 165.9, 143.3, 142.0, 138.0, 130.3, 128.8, 128.3, 128.2, 128.1, 128.0, 127.6, 126.6, 125.3, 124.9, 83.0, 64.5, 62.6, 46.6, 41.5, 23.5, 14.9. HRMS (EI): calcd for $C_{27}H_{27}NO_4$, 429.1940; found, 429.1942.

2-Hydroxy-9-methyl-5,8-dioxo-2-phenyl-3-[(2*R*)-phenylethyl]-(2*R*,3*R*,9*S*)-7-oxa-4-azabicyclo[8.3.1]tetradeca-1(14),10,12-triene (7bB). ^{1}H NMR (300 MHz, $CDCl_3$): δ 7.65−7.52 (m, 4H), 7.49−7.42 (m, 1H), 7.40 (s, 1H), 7.35−7.29 (m, 3H), 7.08 (d, J = 4.7 Hz, 2H), 6.89−6.78 (m, 3H), 6.00 (d, J = 10.2 Hz, 1H), 5.05 (d, J = 11.3 Hz, 1H), 4.45 (dd, J = 10.2 Hz, 2.5 Hz, 1H), 4.34 (d, J = 11.3 Hz, 1H), 3.78 (q, J = 7.0 Hz, 1H), 3.52−3.42 (m, 1H), 1.55 (d, J = 7.0 Hz, 3H), 1.26 (d, J = 7.2 Hz, 3H). ^{13}C NMR (75 MHz, $CDCl_3$): δ 175.0, 165.8, 142.5, 142.3, 142.1, 139.5, 129.5, 128.7, 128.5, 128.0, 127.9, 127.8, 127.4, 126.8, 126.1, 124.5, 81.5, 66.4, 60.7, 47.6, 39.3, 20.2, 16.4. HRMS (EI): calcd for $C_{27}H_{27}NO_4$, 429.1940; found, 429.1941.

2-Hydroxy-9-methyl-5,8-dioxo-2-phenyl-3-[(2*R*)-phenylethyl]-(2*R*,3*S*,9*S*)-7-oxa-4-azabicyclo[8.3.1]tetradeca-1(14),10,12-triene (7bC). ^{1}H NMR (300 MHz, $CDCl_3$): δ 7.52−7.17 (m, 12H), 7.07 (d, J = 8.3 Hz, 2H), 5.50 (d, J = 15.0 Hz, 1H), 5.36 (d, J = 10.6 Hz, 1H), 5.02 (dd, J = 10.6 Hz, 3.2 Hz, 1H), 4.30 (d, J = 15.0 Hz, 1H), 3.87 (q, J = 7.0 Hz, 1H), 3.00−2.90 (m, 1H), 2.24 (br. s, 1H), 1.64 (d, J = 7.0 Hz, 3H), 0.54 (d, J = 7.2 Hz, 3H). ^{13}C NMR (75 MHz, $CDCl_3$): δ 173.7, 167.0, 147.1, 141.5, 139.6, 139.3, 131.6, 128.9, 128.8, 128.5, 128.4, 128.2, 127.1, 126.8, 126.6, 125.5, 84.5, 63.7, 61.5, 46.7, 40.2, 20.1, 16.9. HRMS (EI): calcd for $C_{27}H_{27}NO_4$, 429.1940; found, 429.1949.

2-Hydroxy-9-methyl-5,8-dioxo-2-phenyl-3-[(2*R*)-phenylethyl]-(2*S*,3*R*,9*S*)-7-oxa-4-azabicyclo[8.3.1]tetradeca-1(14),10,12-triene (7bD). ^{1}H NMR (300 MHz, $CDCl_3$): δ 7.57−7.30 (m, 6H), 7.24−7.04 (m, 8H), 6.07 (d, J = 10.5 Hz, 1H), 5.03 (d, J = 13.3 Hz, 1H), 4.77 (dd, J = 10.5 Hz, 4.2 Hz, 1H), 4.24 (d, J = 13.3 Hz, 1H), 3.90 (q, J = 7.2 Hz, 1H), 3.09 (m, 1H), 1.56 (d, J = 7.2 Hz, 3H), 1.19 (d, J = 7.2 Hz, 3H). ^{13}C NMR (75 MHz, $CDCl_3$): δ 173.6, 165.4, 146.9, 142.8, 142.1, 137.2, 130.1, 128.4, 128.4, 128.3, 127.7, 127.2, 126.9, 126.1, 125.2, 124.5, 83.1, 65.2, 59.7, 45.9, 40.1, 19.2, 13.1. HRMS (EI): calcd for $C_{27}H_{27}NO_4$, 429.1940; found, 429.1922.

Isolation of Photoproducts 8A−8D. The mixed fraction containing photoproducts **8A−8D** (which could not be resolved with a reversed phase HPLC column) was separated by HPLC with a semipreparative chiral column (Dancel Chiracel OD, length 25 cm, diameter 1.0 cm) and an *n*-hexane/ethanol mixture (97/3 v/v) as eluent, operated under isocratic conditions at a flow rate of 4 mL min^{-1}. Compounds **8B** and **8C** were obtained as pure products, while **8A** and **8D** were collected together in one fraction, which was finally resolved by a subsequent preparative chromatography (column Kromasil 100, reversed phase C18, 5 μm, length 25 cm, diameter 1.0 cm; eluent methanol/water 60/40 v/v; flow rate 4 mL min^{-1}).

2-Hydroxy-3,10-dimethyl-6,9-dioxo-2,3-diphenyl-(2*S*,3*S*,10*S*)-8-oxa-5-azabicyclo[9.3.1]pentadeca-1(15),11,13-triene (8A). ^{1}H NMR (300 MHz, $CDCl_3$): δ 7.80 (d, J = 8.3 Hz, 1H), 7.62−7.53 (m, 3H), 7.43−7.29 (m, 4H), 7.23−7.10 (m, 4H), 7.04−6.97 (m, 2H), 6.41 (br. s, 1H), 5.30 (d, J = 15.3 Hz, 1H), 4.51 (dd, J = 15.1 Hz, 4.1 Hz, 1H), 4.15 (d, J = 15.3 Hz, 1H), 3.82 (q, J = 7.2 Hz, 1H), 3.32 (dd, J = 15.1 Hz, 3.7 Hz, 1H), 1.40 (d, J = 7.2 Hz, 3H), 1.32 (s, 3H). ^{13}C NMR (75 MHz, $CDCl_3$): δ 173.2, 167.9, 143.9, 143.7, 141.4, 140.2, 129.0, 128.4, 128.2, 128.0, 127.9, 127.8, 127.6, 127.4, 127.3, 126.1, 80.7, 62.7, 51.0, 48.8, 45.2, 22.5, 18.0. HRMS (EI): calcd for $C_{27}H_{27}NO_4$, 429.1940; found, 429.1966.

2-Hydroxy-3,10-dimethyl-6,9-dioxo-2,3-diphenyl-(2*R*,3*R*,10*S*)-8-oxa-5-azabicyclo[9.3.1]pentadeca-1(15),11,13-triene (8B). ^{1}H NMR (300 MHz, $CDCl_3$): δ 7.75 (s, 1H), 7.45 (d, J = 8.0 Hz, 2H), 7.41−7.15 (m, 7H), 7.14−7.01 (m, 2H), 6.90 (d, J = 8.0 Hz, 2H), 6.43 (br. s, 1H), 4.66 (d, J = 15.2 Hz, 1H), 4.52 (d, J = 15.2 Hz, 1H), 4.02 (dd, J = 14.5 Hz, 4.0 Hz, 1H), 3.85 (q, J = 7.0 Hz, 1H), 3.62 (dd, J = 14.5 Hz, 6.0 Hz, 1H), 1.57 (d, J = 7.0 Hz, 3H), 1.34 (s, 3H). ^{13}C NMR (75 MHz, $CDCl_3$): δ 172.8, 167.7, 143.9, 142.2, 139.2, 129.8, 128.2, 127.9, 127.4, 127.4, 127.3, 125.6, 116.7, 81.1, 62.7, 51.2, 48.4, 45.4, 23.0, 15.0. HRMS (EI): calcd for $C_{27}H_{27}NO_4$, 429.1940; found, 429.1937.

2-Hydroxy-3,10-dimethyl-6,9-dioxo-2,3-diphenyl-(2*R*,3*S*,10*S*)-8-oxa-5-azabicyclo[9.3.1]pentadeca-1(15),11,13-triene (8C). ^{1}H NMR (300 MHz, $CDCl_3$): δ 7.92 (s, 1H), 7.46−7.34 (m, 2H), 7.33−7.24 (m, 3H), 7.24−7.12 (m, 8H), 5.46 (m, 1H), 4.63 (d, J = 15.1 Hz, 1H), 4.54 (d, J = 15.1 Hz, 1H), 4.07 (q, J = 7.2 Hz, 1H), 3.95 (dd, J = 14.0 Hz, 3.0 Hz, 1H), 3.62 (dd, J = 14.0 Hz, 8.0 Hz, 1H), 2.78 (s, 1H), 1.66 (d, J = 7.2 Hz, 3H), 1.54 (s, 3H). ^{13}C NMR (75 MHz, $CDCl_3$): δ 172.9, 167.5, 145.2, 144.4, 144.0, 138.6, 129.6, 128.3, 128.1, 127.9, 127.5, 127.4, 127.2, 127.1, 127.0, 125.6, 81.2, 62.7, 51.2, 46.7, 45.9, 21.5, 15.3. HRMS (EI): calcd for $C_{27}H_{27}NO_4$, 429.1940; found, 429.1881.

2-Hydroxy-3,10-dimethyl-6,9-dioxo-2,3-diphenyl-(2*S*,3*R*,10*S*)-8-oxa-5-azabicyclo[9.3.1]pentadeca-1(15),11,13-triene (8D). ^{1}H NMR (300 MHz, $CDCl_3$): δ 7.86 (s, 1H), 7.80 (d, J = 8.0 Hz, 1H), 7.37 (t, J = 7.8 Hz, 1H), 7.25−7.06 (m, 7H), 7.01−6.93 (m, 4H), 5.12 (d, J = 15.3 Hz, 1H), 4.93 (m, 1H), 3.96 (d, J = 15.3 Hz, 1H), 3.91 (dd, J = 10.5, 13.8 Hz, 1H), 3.82 (q, J = 7.0 Hz, 1H), 3.60 (dd, J = 13.8 Hz, 3.3 Hz, 1H), 1.70 (d, J = 7.0 Hz, 3H), 1.57 (s, 3H). ^{13}C NMR (75 MHz, $CDCl_3$): δ 173.4, 167.5, 144.2, 143.8, 142.5, 139.0, 130.3, 128.9, 128.0, 127.6, 127.4, 127.3, 127.2, 127.1, 126.7, 80.1, 62.6, 52.5, 45.8, 44.3, 20.4, 17.3. HRMS (EI): calcd for $C_{27}H_{27}NO_4$, 429.1940; found, 429.1890.

Single-Crystal X-ray Data. Suitable crystals were obtained by slow evaporation of the respective organic solvent at room temperature. Crystal data were collected on a NONIUS KappaCCD2000 diffractometer using OSMIC-graded monochromatic multilayer Cu K_α radiation. The structure was solved by direct methods and refined using SHELX97 (Sheldrick, G. M., University of Göttingen). Non-hydrogen atoms were found by successive full matrix least-squares refinement on F^2. Hydrogen atoms were placed at idealized positions and refined with a riding model. Crystallographic information for compounds **6aB**, **6aD**, **6bC−6bD**, **7aA**, **7bA−7bC**, and **8B−8D** are given in Tables 3 and 4.

Acknowledgment. We acknowledge the financial support by the Spanish Ministry of Education and Science, Madrid (Grant No. CTQ 2004-03811, doctoral fellowship for S.A. and Ramón

y Cajal grant for U.P.). Dedicated to Professor Miguel Yus on the occasion of his 60th birthday.

Supporting Information Available: CCDC 622400 (**6aB**), CCDC 622401 (**6aD**), CCDC 622402 (**6bB**), CCDC 622403 (**6bC**), CCDC 622404 (**6bD**), CCDC 622405 (**7aA**), CCDC 631031 (**7bA**), CCDC 622406 (**7bB**), CCDC 622407 (**7bC**), CCDC 622408 (**8B**), CCDC 622409 (**8C**), and CCDC 622410 (**8D**) contain the supplementary crystallographic data for this paper. These data can be obtained free of charge *via* www.ccdc.cam.ac.uk/data_request/cif or by emailing data_request@ccdc.cam.ac.uk or by contacting The Cambridge Crystallographic Data Centre, 12, Union Road, Cambridge CB2 1EZ, UK. Fax: (+44)-1223-336033. ^{1}H, ^{13}C NMR spectra, NOE data, ORTEP representations of crystal structures, DFT optimized structures and energies of transition states and biradicals, complete ref 85, and CIF files of single-crystal structure determination. This material is available free of charge via the Internet at http://pubs.acs.org.

JA0712827